
JOURNAL OF THE AMERICAN CHEMICAL SOCIETY

Structure and Dynamics of Disulfide Cross-Linked DNA Triple Helices

Scott E. Osborne, Robert J. Cain, and Gary D. Glick*

Contribution from the Department of Chemistry, University of Michigan,
Ann Arbor, Michigan 48109-1055

Received September 18, 1996[⊗]

Abstract: The design, synthesis, and characterization of two disulfide cross-linked intramolecular pyr·pur–pyr triple helices (IV and V) is presented. Placement of a covalent cross-link from the Hoogsteen strand to the Watson–Crick duplex produces two fundamental changes in the cross-linked DNAs relative to the parent sequence. First, formation of the cross-link results in an increase in the apparent pK_a of the Hoogsteen cytosines by 1.5 pK_a units (to 8.6 and 8.3 for IV and V, respectively) with a concomitant increase in thermal stability of ~ 40 °C at pH 7.4. Second, the cross-link enforces the triplex structure over a wide range of solution conditions, including those that are physiologically relevant (e.g., pH 7.4, 155 mM Na^+ , 37 °C). CD and NMR measurements indicate that the cross-link does not significantly perturb the geometry of IV and V relative to their unmodified counterpart. Because the disulfide cross-link effectively prevents conformational heterogeneity associated with pyr·pur–pyr triple helices containing $C^+ \cdot G-C$ base-triplets at neutral pH, constructs possessing this modification can serve as model systems to examine the structural and thermodynamic aspects of triplex formation *in vitro* and to aid in the development of sequences that bind with higher affinity and specificity.

Introduction

Triple helix formation can occur when either a (homo)pyrimidine strand binds parallel to the purine strand of a (homo)purine–(homo)pyrimidine (pyr·pur–pyr) duplex via Hoogsteen $C^+ \cdot G-C$ and $T \cdot A-T$ base-pairing, or when a (homo)purine strand binds antiparallel to the purine strand of a (homo)purine–(homo)pyrimidine (pur·pur–pyr) duplex via Hoogsteen $G \cdot G-C$ and $A \cdot A-T$ base-pairing.¹ In both cases, third strand binding is dependent on a variety of parameters including, base composition, sequence, temperature, and buffer.² For example, in native pyr·pur–pyr triple helices, protonation of the Hoogs-

teen cytosine in $C^+ \cdot G-C$ base triplets is required to form the second Hoogsteen hydrogen bond. Consequently, triplexes containing $C^+ \cdot G-C$ base triplets usually unfold above pH 6–7.^{3,4}

Several methods have been developed to increase the con-

(2) (a) Plum, G. E.; Pilch, D. S.; Singleton, S. F.; Breslauer, K. J. *Annu. Rev. Biophys. Biomol. Struct.* **1995**, *24*, 319–350. (b) Wilson, W. D.; Hopkins, H. P.; Mizan, S.; Hamilton, D. D.; Zon, G. *J. Am. Chem. Soc.* **1994**, *116*, 3607–3608. (c) Kiessling, L. L.; Griffin, L. C.; Dervan, P. B. *Biochemistry* **1992**, *31*, 2829–2834. (d) Pilch, D. S.; Levenson, C.; Shafer, R. H. *Proc. Natl. Acad. Sci. U.S.A.* **1990**, *87*, 1942–1946. (e) Moser, H. E.; Dervan, P. B. *Science* **1987**, *238*, 645–650.

(3) The pK_a of the Hoogsteen N^3 -cytosine protons in triple helices is between 5.0 and 7.0: (a) Singleton, S. F.; Dervan, P. B. *Biochemistry* **1992**, *31*, 10995–11003. (b) Callahan, D. E.; Trapane, T. L.; Miller, P. S.; Ts'o, P. O. P.; Kan, L.-S. *Biochemistry* **1991**, *30*, 1650–1655.

(4) Triplex sequences containing $^5mC^+ \cdot G-C$ base-triplets in place of $C^+ \cdot G-C$ base-triplets have been observed at physiologically relevant conditions. For examples, see: (a) Lin, S.-B.; Kao, C.-F.; Lee, S.-U.; Kan, L.-S. *Anti-Cancer Drug Design* **1994**, *9*, 1–8. (b) Lee, J. S.; Woodsworth, M. L.; Latimer, L. J. P.; Morgan, A. R. *Nucleic Acids Res.* **1984**, *12*, 6603–6614.

* Address correspondence to this author. Phone (313)764-4548; fax (313)764-8815; e-mail gglick@umich.edu.

[⊗] Abstract published in *Advance ACS Abstracts*, February 1, 1997.

(1) For recent reviews of pyr·pur–pyr and pur·pur–pyr triplexes, see: (a) Radhakrishnan, I.; Patel, D. J. *Biochemistry* **1994**, *33*, 11405–11416. (b) Hélène, C. *Curr. Opin. Biotechnol.* **1993**, *4*, 29–36. (c) Dervan, P. B. *Nature* **1992**, *359*, 87–88. (d) Hélène, C. *Anti-Cancer Drug Design* **1991**, *6*, 569–584.

formational stability of pyr·pur–pyr triple helices (primarily for use *in vivo*),⁵ and these methods can be placed within two groups. The first group involves strengthening the interactions that stabilize triplex formation through chemical modifications to the Hoogsteen cytosine.^{3,6} The second method for stabilizing triplexes centers on attaching, either covalently or noncovalently, the labile Hoogsteen strand to the double-helix.⁷ For example, intercalating groups (e.g., acridine and benzopyridoindole) have been covalently tethered to the Hoogsteen strand so that upon binding the intercalator inserts into the duplex and locks the third strand within the major groove.⁸ In some cases these intercalators contain photolabile reactive groups so that, upon intercalation and photolysis, the third strand becomes covalently cross-linked to the Watson–Crick strand.⁹ However, the effects of these cross-links on the stability of the modified triplexes have not been addressed.

Several examples of covalent cross-links to stabilize nucleic acid structure have recently been described.¹⁰ Our laboratory has contributed to this area of research with the development of a flexible synthetic methodology for incorporating disulfide cross-links¹¹ into DNA hairpins,¹² duplexes,¹³ non-ground-state

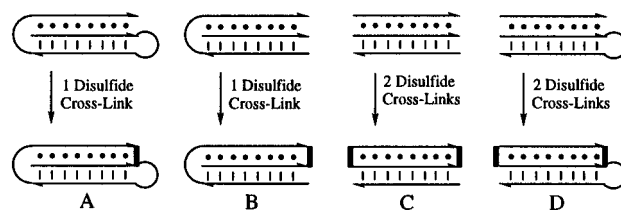


Figure 1. Pyr·pur–pyr triple helices consisting of one (A), two (B and C), and three (D) oligonucleotide strand(s). These structures are formed by (A) folding of a single strand into an intramolecular triple helix; (B) addition of complementary homopurine strand to a palindromic homopyrimidine sequence; (C) addition of a complementary homopyrimidine strand to a homopyrimidine/homopurine hairpin; and (D) mixing a 2:1 stoichiometric ratio of homopyrimidine and homopurine strands, respectively. Arrows denote the 3' end, dashes represent Watson–Crick hydrogen bonding, dots represent Hoogsteen hydrogen bonding, and the bold line(s) indicates cross-link(s). Of the four possible ways to form a pyr·pur–pyr triplex structure, two of these (A and B) should only require one cross-link to tie the Hoogsteen strand to the major groove because the (oligo)nucleotide loop connecting the Hoogsteen strand and the Watson–Crick pyrimidine strand should effectively function as a second cross-link. Although not presented in this illustration, triplexes B and D can also form iso-structures in which the (oligo)nucleotide loop is on the opposite end of the helix.

(5) For a comprehensive review of these methods, see: (a) Sun, J.-S.; Hélène, C. *Curr. Opin. Struct. Biol.* **1993**, *3*, 345–356. (b) Thuong, N. T.; Hélène, C. *Angew. Chem., Int. Ed. Engl.* **1993**, *32*, 666–690.

(6) (a) Voegel, J. J.; Benner, S. A. *J. Am. Chem. Soc.* **1994**, *116*, 6929–6930. (b) Xiang, G.; Soussou, W.; McLaughlin, L. W. *J. Am. Chem. Soc.* **1994**, *116*, 11155–11156. (c) Koh, J. S.; Dervan, P. B. *J. Am. Chem. Soc.* **1992**, *114*, 1470–1478. (d) Egholm, M.; Buchardt, O.; Nielsen, P. E.; Berg, R. H. *J. Am. Chem. Soc.* **1992**, *114*, 1895–1897. (e) Roberts, R. W.; Crothers, D. M. *Science* **1992**, *258*, 1463–1466. (f) Xodo, L. E.; Manzini, G.; Quadrifoglio, F.; van der Marel, G. A.; van Boom, J. H. *Nucleic Acids Res.* **1991**, *19*, 5625–5631. (g) Ono, A.; Ts'o, P. O. P.; Kan, L.-S. *J. Am. Chem. Soc.* **1991**, *113*, 4032–4033. (h) Matteucci, M.; Lin, K.-Y.; Butcher, S.; Moulds, C. *J. Am. Chem. Soc.* **1991**, *113*, 7767–7768. (i) Povsic, T. J.; Dervan, P. B. *J. Am. Chem. Soc.* **1989**, *111*, 3059–3061.

(7) For a review of these methods, see: Hélène, C. *Pure Appl. Chem.* **1994**, *66*, 663–669.

(8) (a) Cassidy, S. A.; Strekowski, L.; Wilson, W. D.; Fox, K. R. *Biochemistry* **1994**, *33*, 15338–15347. (b) Wilson, W. D.; Tanious, F. A.; Mizan, S.; Yao, S.; Kiselyov, A. S.; Zon, G.; Strekowski, L. *Biochemistry* **1993**, *32*, 10614–10621. (c) Mergny, J. L.; Duval-Valentin, G.; Nguyen, C. H.; Perrouault, L.; Faucon, B.; Rougée, M.; Montenay-Garestier, T.; Bisagni, E.; Hélène, C. *Science* **1992**, *256*, 1681–1684. (d) Giovannangeli, C.; Thuong, N. T.; Hélène, C. *Nucleic Acids Res.* **1992**, *20*, 4275–4281. (e) Collier, D. A.; Thuong, N. T.; Hélène, C. *J. Am. Chem. Soc.* **1991**, *113*, 1457–1458. (f) Perrouault, L.; Asseline, U.; Rivalle, C.; Thuong, N. T.; Bisagni, E.; Giovannangeli, C.; Le Doan, T.; Hélène, C. *Nature* **1990**, *344*, 358–360. (g) Sun, J.-S.; François, J.-C.; Montenay-Garestier, T.; Saison-Behmoaras, T.; Roig, V.; Thuong, N. T.; Hélène, C. *Proc. Natl. Acad. Sci. U.S.A.* **1989**, *86*, 9198–9202. (h) Asseline, U.; Thuong, N. T.; Hélène, C. *J. Biol. Chem.* **1985**, *260*, 8936–8941.

(9) (a) Praseuth, D.; Perrouault, L.; Le Doan, T.; Chassignol, M.; Thuong, N. T.; Hélène, C. *Proc. Natl. Acad. Sci. U.S.A.* **1988**, *85*, 1349–1353. (b) Le Doan, T.; Perrouault, L.; Praseuth, D.; Habhou, N.; Decout, J.-L.; Thuong, N. T.; Lhomme, J.; Hélène, C. *Nucleic Acids Res.* **1987**, *15*, 7749–7760.

(10) For examples, see: (a) Sigurdsson, S. T.; Rink, S. M.; Hopkins, P. B. *J. Am. Chem. Soc.* **1993**, *115*, 12633–12634. (b) Cowart, M.; Benkovic, S. J. *Biochemistry* **1991**, *30*, 788–796. (c) Kirchner, J. J.; Hopkins, P. B. *J. Am. Chem. Soc.* **1991**, *113*, 4681–4682. (d) Borowy-Borowski, H.; Lipman, R.; Chowdary, D.; Tomasz, M. *Biochemistry* **1990**, *29*, 2992–2999. (e) Pinto, A. L.; Lippard, S. J. *Biochim. Biophys. Acta* **1985**, *780*, 167–180.

(11) For other examples of disulfide cross-links incorporated into nucleic acids, see: (a) Gao, H.; Yang, M.; Cook, A. F. *Nucleic Acids Res.* **1995**, *23*, 285–292. (b) Chaudhuri, N. C.; Kool, E. T. *J. Am. Chem. Soc.* **1995**, *117*, 10434–10442. (c) Wolfe, S. A.; Ferentz, A. E.; Grantcharova, V.; Churchill, M. E. A.; Verdine, G. L. *Chem. Biol.* **1995**, *2*, 213–221. (d) Ferentz, A. E.; Keating, T. A.; Verdine, G. L. *J. Am. Chem. Soc.* **1993**, *115*, 9006–9014. (e) Milton, J.; Connolly, B. A.; Nikiforov, T. T.; Cosstick, R. J. *Chem. Soc., Chem. Commun.* **1993**, 779–780. (f) Wolfe, S. A.; Verdine, G. L. *J. Am. Chem. Soc.* **1993**, *115*, 12585–12586.

(12) Glick, G. D. *J. Org. Chem.* **1991**, *56*, 6746–6747.

(13) Osborne, S. E.; Völker, J.; Stevens, S. Y.; Breslauer, K. J.; Glick, G. D. *J. Am. Chem. Soc.* **1996**, *118*, 11993–12003.

structures,¹⁴ and RNA.¹⁵ Unlike other methodologies, these cross-links impart increased stability against denaturation induced by changes in temperature, ionic strength, and [nucleic acid] without perturbing native helical geometry.¹³ Recently we have expanded this chemistry to include triple helices and in previous experiments demonstrated that positioning a cross-link at the terminus of an intramolecular triplex increases thermal stability relative to the unmodified oligonucleotide.¹⁶ Here we present the design of two disulfide cross-linked intramolecular pyr·pur–pyr triple helices, synthesis of the modified nucleosides used to form the cross-link, and structural characterization of these constructs.¹⁷ We find that the cross-link does not appear to disrupt native geometry. Moreover, the cross-link increases the apparent pK_a of the third strand by as much as 1.5 units relative to the unmodified triplex so that the cross-linked triplex structures remain conformationally homogeneous at pH 7.4 up to 50 °C. We discuss the results in terms of previous efforts to stabilize triple helices and potential applications of these novel constructs.

Results

Design and Synthesis. Previous studies in our laboratory have demonstrated that positioning a cross-link between the terminal bases on a helix imparts increased thermal stability of the construct in question.^{12–14} Similarly, placing a cross-link between the terminus of the Hoogsteen strand and the Watson–Crick purine strand on a triplex should lock the labile third strand into the major groove, leading to an increase in stability against pH- and thermal-induced denaturation. We chose to test this hypothesis using an intramolecular triplex rather than an intermolecular construct because the former should require only one cross-link to link the Hoogsteen strand to the Watson–Crick duplex (Figure 1).¹⁸ To place a cross-link between the

(14) Glick, G. D.; Osborne, S. E.; Knitt, D. S.; Marino, J. P., Jr. *J. Am. Chem. Soc.* **1992**, *114*, 5447–5448.

(15) (a) Goodwin, J. T.; Osborne, S. E.; Scholle, E. J.; Glick, G. D. *J. Am. Chem. Soc.* **1996**, *118*, 5207–5215. (b) Goodwin, J. T.; Glick, G. D. *Tetrahedron Lett.* **1994**, *35*, 1647–1650.

(16) Goodwin, J. T.; Osborne, S. E.; Swanson, P. C.; Glick, G. D. *Tetrahedron Lett.* **1994**, *35*, 4527–4530.

(17) The thermodynamic stability of the cross-linked triplexes is presented in another article: Völker, J.; Osborne, S. E.; Glick, G. D.; Breslauer, K. J. *Biochemistry*, in press.

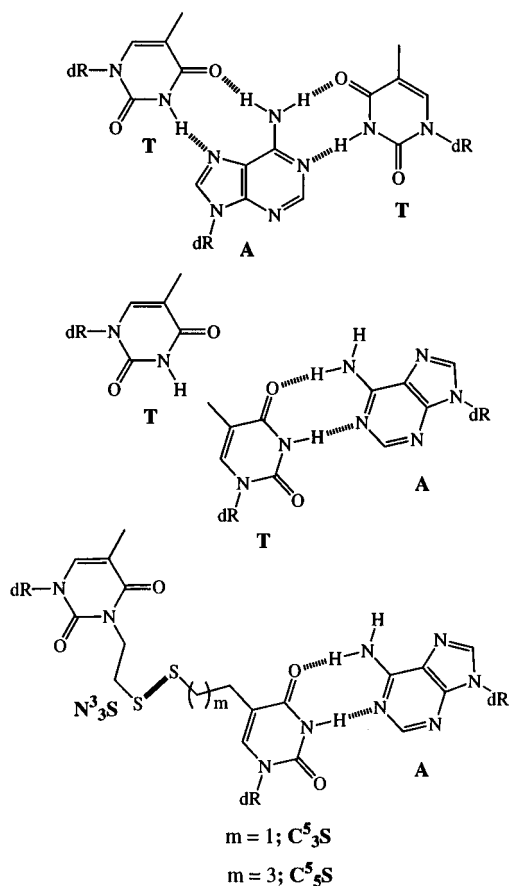


Figure 2. Illustration of base triplets T·A–T (top), T·T–A (middle), and N³·S·C⁵·S–A (bottom). The Hoogsteen strand lies within the major groove of the double-helix parallel to the Watson–Crick purine strand (dR = deoxyribose, dashes = Watson–Crick hydrogen bonding, dots = Hoogsteen hydrogen bonding).

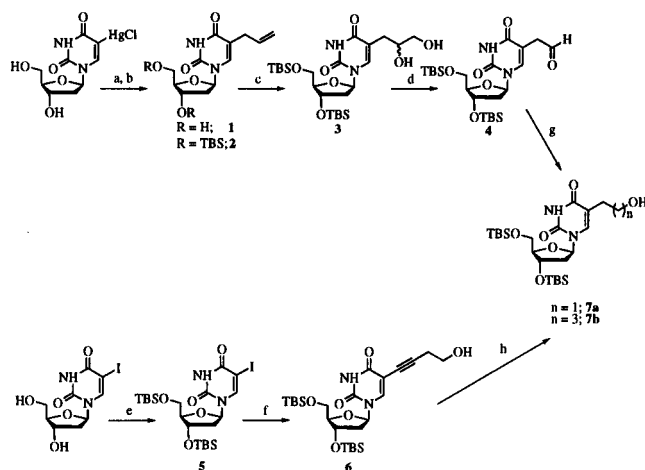
Hoogsteen and Watson–Crick strands, sites of chemical modification on the terminal bases must first be identified. Canonical T·A and C⁺·G Hoogsteen base-pairing does not provide loci for facile modification. However, in a T·T–A triplet, the N³-position on the Hoogsteen thymidine and the C⁵-position of the Watson–Crick thymidine converge (Figure 2) and the N³- and C⁵-positions on thymidine can be readily modified to contain thiol tethers.^{12,19} Therefore, we designed a cross-link to span these two positions using a C⁵-alkyl thiol modified thymidine (C⁵_nS; where *n* = the number of atoms in the linker, including thiol)²⁰ and N³-(thioethyl)thymidine (N³₃S), which we have previously described (Figure 2).^{12–14} To study the effect of linker length on the stability conferred by cross-linking, two different lengths of alkylthiol tethers at the C⁵-position of the Watson–Crick thymidine were synthesized (*n* = 3 or 5) so that a cross-link with N³₃S results in linker lengths of six or eight atoms.²¹

Synthesis of the C⁵-thiol-modified nucleosides was accomplished using chemistry previously developed to modify the

(18) For examples of intramolecular pyr·pur–pyr triple helices, see: (a) Plum, G. E.; Breslauer, K. J. *J. Mol. Biol.* **1995**, *248*, 679–695. (b) Völker, J.; Botes, D. P.; Lindsey, G. G.; Klump, H. H. *J. Mol. Biol.* **1993**, *230*, 1278–1290. (c) Radhakrishnan, I.; Gao, X.; de los Santos, C.; Live, D.; Patel, D. J. *Biochemistry* **1991**, *30*, 9022–9030. (d) Sklenář, V.; Feigon, J. *Nature* **1990**, *345*, 836–838. (e) Häner, R.; Dervan, P. B. *Biochemistry* **1990**, *29*, 9761–9765.

(19) (a) Telser, J.; Cruickshank, K. A.; Morrison, L. E.; Netzel, T. L. *J. Am. Chem. Soc.* **1989**, *111*, 6966–6976. (b) Prober, J. M.; Trainor, G. L.; Dam, R. J.; Hobbs, F. W.; Robertson, C. W.; Zagursky, R. J.; Cocuzza, A. J.; Jensen, M. A.; Baumeister, K. *Science* **1987**, *238*, 336–341. (c) Langer, P. R.; Waldrop, A. A.; Ward, D. C. *Proc. Natl. Acad. Sci. U.S.A.* **1981**, *78*, 6633–6637.

Scheme 1. Synthesis of the C⁵ Three- and Five-Atom Alcohol^a



^a TBS = *tert*-butyldimethylsilyl. (a) PdCl₂, LiCl, MeOH, allyl chloride (78% yield); (b) imidazole, DMF, TBSCl (78% yield); (c) OsO₄, *N*-methylmorpholine *N*-oxide, acetone, H₂O (82% yield); (d) NaIO₄, *p*-dioxane, H₂O (97% yield); (e) imidazole, DMF, TBSCl (92% yield); (f) but-3-yn-1-ol, DMF, Et₃N, CuI, (Ph₃P)₄Pd (79% yield); (g) NaBH₄, MeOH (68% yield); (h) H₂ (35 psi), 10% Pd(C), MeOH (71% yield).

C⁵-position of 2'-deoxyuridine (Scheme 1).¹⁹ Briefly, the C⁵₃S monomer was synthesized via palladium-catalyzed coupling²² of 5-chloromercuri-2'-deoxyuridine²³ with allyl chloride (2). After protection of the hydroxyl groups as silyl ethers, the terminal olefin was oxidized to the corresponding aldehyde,²⁴ and then reduced to the requisite C⁵ three-atom alcohol (7a). C⁵₅S was synthesized from a palladium-catalyzed coupling²⁵ of 5-iodo-2'-deoxyuridine with 3-buten-1-ol, followed by hydrogenation to yield the saturated C⁵ five-atom alcohol (7b).²⁶ The hydroxyl groups on 7a and 7b were activated as mesylates and displaced with thiobenzoic acid (Scheme 2). After removal of the silyl protecting groups, the 5'-hydroxyl group was protected as a 4,4-dimethoxytrityl ether, and the benzoyl protecting group on the thiol was exchanged to the *tert*-butyl mixed disulfide using 1-(*tert*-butylthio)-1,2-hydrazinedicarboxymorpholine.²⁷ Lastly, the 3'-hydroxyl group was activated for solid-phase synthesis as the *N,N*-diisopropyl-β-cyanoethyl phosphoramidite (13a and 13b).²⁸

The optimal pH for air oxidation of thiols to form disulfide bonds generally is above the pK_a of the thiol of interest (~8.5),²⁹ and, in the presence of divalent metals like Mg²⁺, this reaction

(20) Goodwin, J. T.; Glick, G. D. *Tetrahedron Lett.* **1993**, *34*, 5549–5552.

(21) A linker length of four atoms was synthesized (C⁵₄S); however, this nucleoside degrades upon removal of the thiol-protecting group. Synthesis of C⁵₄S was performed as previously described: Bradley, D. H.; Hanna, M. M. *Tetrahedron Lett.* **1992**, *33*, 6223–6226.

(22) Ruth, J. L.; Bergstrom, D. E. *J. Org. Chem.* **1978**, *43*, 2870–2876.

(23) Dreyer, G. B.; Dervan, P. B. *Proc. Natl. Acad. Sci. U.S.A.* **1985**, *82*, 968–972.

(24) (a) Fiandor, J.; Tam, S. Y. *Tetrahedron Lett.* **1990**, *31*, 597–600. (b) Vedejs, E.; Dent, W. H., III; Gapinski, D. M.; McClure, C. K. *J. Am. Chem. Soc.* **1987**, *109*, 5437–5446.

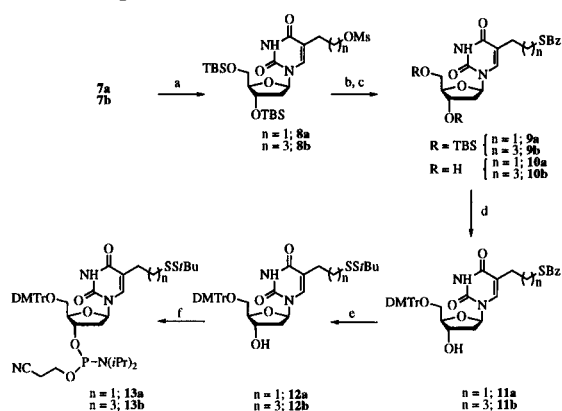
(25) Hobbs, F. W., Jr. *J. Org. Chem.* **1989**, *54*, 3420–3422.

(26) Gibson, K. J.; Benkovic, S. J. *Nucleic Acids Res.* **1987**, *15*, 6455–6467.

(27) (a) Wünsch, E.; Moroder, L.; Romani, S. *Hoppe-Seyler's Z. Physiol. Chem.* **1982**, *363*, 1461–1464. (b) Bock, H.; Kroner, J. *Chem. Ber.* **1966**, *99*, 2039–2051.

(28) (a) Gough, G. R.; Bruden, M. J.; Gilham, P. T. *Tetrahedron Lett.* **1981**, *22*, 4177–4180. (b) Beaucage, S. L.; Caruthers, M. H. *Tetrahedron Lett.* **1981**, *22*, 1859–1862.

(29) Lamoureux, G. V.; Whitesides, G. M. *J. Org. Chem.* **1993**, *58*, 633–641 and references therein.

Scheme 2. Synthesis of C^5 Thiol Modified (C^5_nS) *tert*-Butyl Protected Phosphoramidites^a

^a TBS = *tert*-butyldimethylsilyl; Ms = methanesulfonyl; Bz = benzoyl; DMTr = 4,4'-dimethoxytrityl. (a) MsCl, CH₂Cl₂, pyridine (88% yield, **8a**; 92% yield, **8b**); (b) DMF, Et₃N, thiobenzoic acid (86% yield, **9a**; 92% yield, **9b**); (c) *n*-tetrabutylammonium fluoride, THF (90% yield, **10a**; 100% yield, **10b**); (d) pyridine, DMTrCl (75% yield, **11a**; 59% yield, **11b**); (e) 1-(*tert*-butylthio)-1,2-hydrazinedicarboxymorpholide, LiOH·H₂O, CH₃OH, THF, (90% yield, **12a**; 69% yield, **12b**); (f) *N,N*-diisopropylethylamine, CH₂Cl₂, chloro-*N,N*-diisopropylamino- β -cyanoethylphosphine (74% yield, **13a**; 94% yield, **13b**).

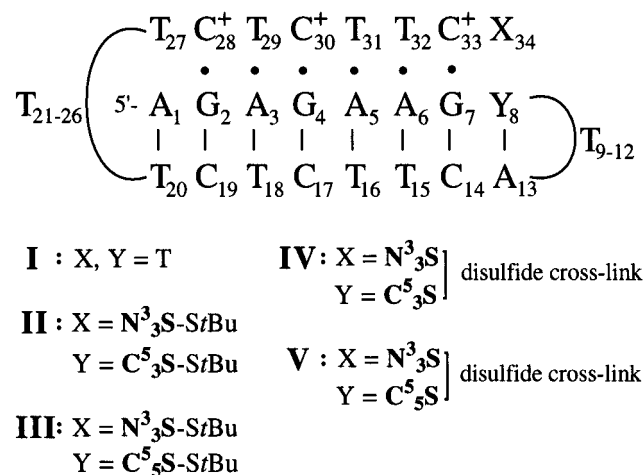


Figure 3. Sequence and numbering scheme of the wild-type, *tert*-butyl protected, and disulfide cross-linked intramolecular DNA triple helices.

can proceed at neutral pH.³⁰ At the pK_a of many thiols, triple helices containing C^+G-C base triplets are unfolded because the N^3 -position of cytosine is not protonated.³ To form a disulfide cross-link in a pyr-pur-pyr triple helix, it is necessary to identify a sequence that (partly) folds into a triplex at a pH where cross-link formation readily proceeds. Recently, Häner and Dervan reported a 34-base-long oligonucleotide that folds intramolecularly into a triple helix that remains partially folded in a triplex conformation up to pH 7.5 at 24 °C in buffer containing 25 mM Mg²⁺.^{18c} Therefore, a disulfide cross-link can, in principle, form under the conditions needed to fold a suitably modified variant of this oligonucleotide (Figure 3; sequence I).

Incorporation of the thiol-modified N^3S and C^5_nS monomers into I was achieved via automated solid-phase DNA synthesis using standard coupling protocols with an average stepwise coupling efficiency of >98.5%. Removal of the phosphate and base protecting groups followed by reversed-phase HPLC

purification provided *tert*-butyl disulfide containing sequences II and III in 34–42% yield (based on a 1 μ mol synthesis; Figure 3). Optical melting studies as a function of pH show that I partly exists in the triple helix conformation at 25 °C and pH 7.25 in phosphate-buffered saline (PBS)³¹ containing MgCl₂ (5 mM).^{16,32} In addition, UV denaturation profiles of II and III are nearly superimposable with I suggesting that the modification does not disrupt binding of the third strand prior to cross-link formation (data not shown).³³ To form the cross-link, the *tert*-butyl thiol protecting groups on II and III were removed with dithiothreitol (DTT), and the reduced DNAs were purified by reversed-phase HPLC. The reduced oligomers were dissolved in PBS (pH 7.25, 5 mM MgCl₂) and vigorously stirred at room temperature while exposed to air. After 24 h, starting material was not observed by HPLC and aliquots from the reaction mixtures tested negative with Ellman's reagent. Cross-linked DNA samples were purified by reversed-phase HPLC to give IV and V in ~28% isolated overall yield (based on a 1 μ mol synthesis; ~75% yield from sequences II and III). Enzymatic nucleoside composition analysis confirmed incorporation of the modified bases and formation of the cross-link, and native and denaturing polyacrylamide gel electrophoresis (PAGE) indicated that the structure formed is a monomolecular single-stranded triple helix (data not shown).

Circular Dichroism Studies. Circular dichroism (CD) spectroscopy was used to monitor triplex formation for I–V. At pH 8.0 and 20 °C, the CD spectrum of I is characteristic of a B–DNA duplex displaying a large positive elliptic signal at 278 nm, a negative band at 248 nm, and positive bands at 221 nm and 213 nm.^{34,35} As the pH is lowered from 8.0 to 5.0, the positive signal at 278 nm red shifts to 280 nm concomitant with a reduction in amplitude, whereas the negative band at 248 nm red shifts to 255 nm. In addition, both positive signals at 213 nm and 221 nm undergo a red shift to 215 nm and 235 nm, respectively, and switch from positive to negative ellipticity, until they reach a minimum at pH 6.0. This pH induced change in the CD spectrum is characteristic of a transition from a hairpin to triple helix structure.^{18a,36} Based on the midpoint of the pH induced transition at 215 nm, we estimate that the apparent pK_a of the N^3 -cytosines in this sequence is about 7.1, which is consistent with previously published pK_a values for intramolecular triple helices (Figure 4).^{18a,37}

Analysis of the CD spectra for thiol-modified sequences II and III reveals no significant differences in the shape of the curves or the pH-dependence relative to I.³⁵ The magnitude of the negative signals present in II and III at 215 nm is slightly larger than that observed for I; however, analysis of sequences that contain either C^5_nS at T₈ or N^3S at T₃₄ suggests that the increased elliptic signal at 215 nm is due to the modification at

(31) PBS refers to NaCl (8 g), KCl (0.2 g), Na₂HPO₄ (1.44 g), and KH₂PO₄ (0.24 g) dissolved in H₂O (1 L): Sambrook, J.; Fritsch, E. F.; Maniatis, T. *Molecular Cloning: A Laboratory Manual*, 2nd ed.; Cold Spring Harbor Laboratory Press: Plainview, NY, 1989; Vol. 3, p B.12.

(32) Similar melting profiles were obtained in PBS containing 25 mM Mg²⁺; however, Mg²⁺ salts precipitate as the samples are heated. Therefore, PBS buffers containing 0.5 mM and 5.0 mM Mg²⁺ were used throughout the remaining studies.

(33) Under anaerobic conditions the reduced forms of II and III display similar UV and CD spectra as the *tert*-butyl protected sequences. Because the *tert*-butyl forms of these sequences cannot oxidatively cross-link, they are easier to manipulate and therefore were used in the remaining studies as models for the reduced triplex sequences.

(34) Ivanov, V. I.; Minchenkova, L. E.; Schyolkina, A. K.; Poletayev, A. I. *Biopolymers* **1973**, *12*, 89–110.

(35) See supporting information.

(36) Manzini, G.; Xodo, L. E.; Gasparotto, D.; Quadrioglio, F.; van der Marel, G. A.; van Boom, J. H. *J. Mol. Biol.* **1990**, *213*, 833–843.

(37) The apparent pK_a of intermolecular triplexes containing C^+G-C base-triplets is between 5.0 and 6.0,³ whereas intramolecular triplexes display apparent pK_a values closer to 7.0.^{18a}

(30) (a) Cullis, C. F.; Trimm, D. L. *Discuss. Faraday Soc.* **1968**, *44*, 144–149. (b) Wallace, T. J. *J. Org. Chem.* **1966**, *31*, 3071–3074.

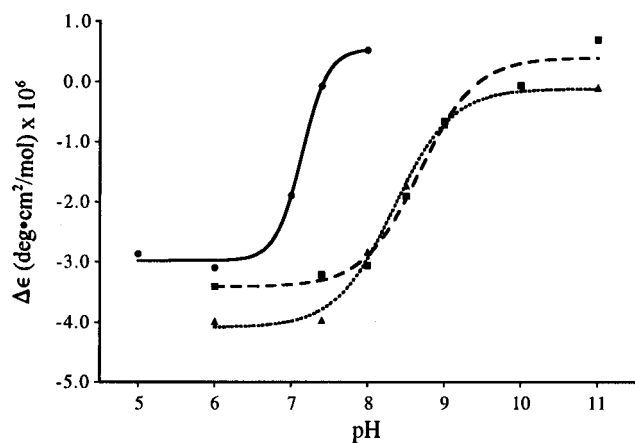


Figure 4. $\Delta\epsilon$ vs pH for I (●), IV (■), and V (▲) measured at 20 °C in PBS buffer with 0.5 mM MgCl_2 . Approximate $\text{p}K_a$ values of the Hoogsteen N^3 -cytosines are defined as the midpoint from the sigmoidal curve to the data points shown,^{18a} and are 7.1 for I, 8.6 for IV, and 8.3 for V.

T_8 (data not shown). This increase in ellipticity may either be due to local changes in the hairpin structure caused by C_5^{S} or to differences in the stacking interactions between these sequences and I. Regardless, the CD spectra of II and III indicate that the thiol-modified thymidines do not disrupt the global geometry of this triplex, do not alter the pH induced hairpin-triplex transition, and do not lower the apparent $\text{p}K_a$ value of the Hoogsteen N^3 -cytosine residues.

The CD spectrum of IV is essentially independent of pH up to 8.0.³⁵ The observation of a strong negative signal at 215 nm in these spectra suggests that the DNA is in a triple helical conformation.^{18a,36} Only when the pH is greater than 8.5 does this band increase in ellipticity, indicating that the third strand is not bound in the major groove of the hairpin. These observations suggest that the cross-link stabilizes the triple helix conformation toward pH induced denaturation, and, based on a plot of $\Delta\epsilon_{215}$ vs pH for IV, the apparent $\text{p}K_a$ of the cytosine residues is about 8.6, which is 1.5 $\text{p}K_a$ units higher than that measured for I (Figure 4). From the similarity in the overall shape of the CD curves of IV relative to I, it appears that the cross-link does not disrupt the overall geometry of the triplex. The negative signal at 215 nm in the CD spectra of IV is greater in the magnitude than that observed for II and III. This decrease in ellipticity results in part from the base modification on the purine strand at T_8 and also from enforced binding of the third strand in the major groove by the cross-link, which effectively increases the "triple helical" character.

The pH-dependent CD spectra for triplex V follows the same trends as for IV except that the increase in ellipticity begins to occur at a lower pH than IV (see Figure 4). As a result, the apparent $\text{p}K_a$ of this triplex is about 0.3 unit lower than IV, suggesting that the longer linker in V does not stabilize the triplex structure toward pH-induced denaturation to the same degree as the shorter cross-link in IV. Alternatively, it is possible that the observed decrease in pH-induced stabilization for V may be from conformational destabilization induced by the longer linker. Discriminating between these two possibilities, however, is outside the scope of the CD data. Lastly, hysteresis is not observed upon titrating sequences I–V from pH 8.0 to 6.0, suggesting that the $\text{p}K_a$ values obtained from the CD spectra represent thermodynamic rather than kinetic parameters.

Between 10 °C and 40 °C, the CD spectrum of IV remains essentially unchanged, and the strong negative elliptic signal at 215 nm suggests that this construct is in the triplex conforma-

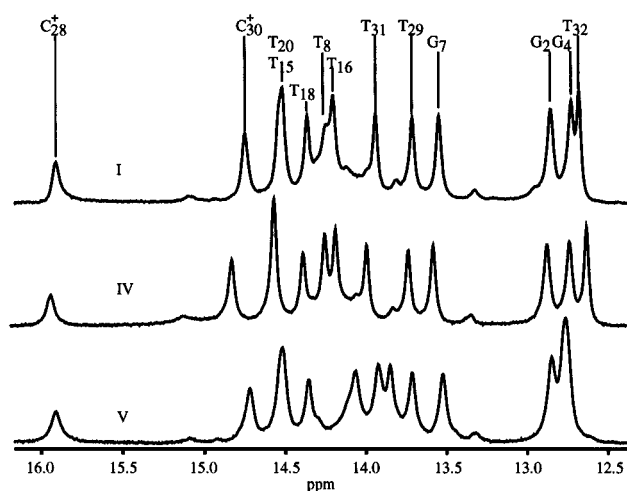


Figure 5. 500 MHz ^1H NMR spectra of the imino proton region of I, IV, and V at pH 6.0 and 1 °C in PBS buffer (90% $\text{H}_2\text{O}/10\%$ D_2O) with MgCl_2 (0.5 mM).

tion.³⁵ Above 40 °C, the ellipticity at 215 nm begins to increase until it reaches a maximum value at 80 °C. The thermal denaturation pathway observed here is consistent with UV and differential scanning calorimetry (DSC) data for IV under similar buffer conditions.³⁸ More importantly, these results indicate that the cross-link in IV provides a conformationally homogeneous triplex under physiologically relevant conditions (pH 7.4, 155 mM Na^+ , 37 °C).

NMR Studies. At pH 6.0 the ^1H NMR spectrum of I contains 13 distinct resonances that fall between 12.5 and 16.0 ppm (Figure 5). Based on previous NMR studies of DNA triple helices,^{18c,d,39} this observation indicates that I is in the triplex conformation and is consistent with our CD and PAGE analyses. Assignment of the imino proton resonances was performed as previously described.^{18d,40} Briefly, the two distinct sets of sequential NOE connectivities in the exchangeable NOESY spectrum that belong to the Watson–Crick guanosine and thymidine imino protons and the Hoogsteen thymidine and protonated cytosine imino protons were located first. Assignment of the Hoogsteen set of connectivities was determined by locating the protonated cytosine imino protons involved in Hoogsteen hydrogen bonding to the Watson–Crick guanosine N^7 based on their characteristically downfield (9.0–10.5 ppm) NOESY cross-peak with the cytosine amino protons. The remaining Hoogsteen imino protons that belong to the Hoogsteen thymidine imino protons were then assigned based on their position within the NOE connectivity (Table 1). The Watson–Crick connectivities were assigned by first designating the resonances at 12.8 and 12.9 ppm as guanosine imino protons based on their characteristic upfield chemical shift. This asymmetry then allowed for the complete assignment of the remaining Watson–Crick imino protons.⁴¹

Similar to I, the imino proton spectra of the cross-linked triplexes at pH 6.0 also show 13 distinct resonances (Figure 5). These resonances were assigned in a similar manner as I (Table I). In general, the imino proton chemical shifts of IV are very

(38) At pH 7.4, the T_m of the triplex–hairpin transition for I and IV is 11.3 °C and 52.0 °C, respectively, and the T_m of the hairpin–coil transition for I and IV is 65.5 °C and 58.5 °C, respectively.¹⁷

(39) Kan, L.-S.; Callahan, D. E.; Trapane, T. L.; Miller, P. S.; Ts'o, P. O. P.; Huang, D. H. *J. Biomol. Struct. Dyn.* **1991**, 8, 911–933.

(40) de los Santos, C.; Rosen, M.; Patel, D. *Biochemistry* **1989**, 28, 7282–7289.

(41) Although it is possible to assign the Watson–Crick imino protons with the opposite polarity (e.g., T_8 is actually T_{20}), comparing chemical shifts of corresponding protons for I, IV, and V indicates this is not the case since only the imino protons adjacent to the cross-link vary (Table I).

Table 1. Chemical Shifts (ppm) of H-Bonded Imino Proton Resonances at pH 6.0 and 1 °C^a

base-pair	I	IV	V
A ₁ •T ₂₀	14.55	14.56	14.54
G ₂ •C ₁₉	12.86	12.86	12.86
A ₃ •T ₁₈	14.37	14.38	14.37
G ₄ •C ₁₇	12.74	12.72	12.76
A ₅ •T ₁₆	14.21	14.24	14.07
A ₆ •T ₁₅	14.52	14.55	14.52
G ₇ •C ₁₄	13.55	13.56	13.53
Y ₈ •A ₁₃	14.26	14.17	13.93
C ⁺ ₂₈ -G ₂	15.92	15.92	15.92
T ₂₉ -A ₃	13.72	13.72	13.72
C ⁺ ₃₀ -G ₄	14.76	14.81	14.72
T ₃₁ -A ₅	13.95	13.98	13.86
T ₃₂ -A ₆	12.68	12.61	12.79

^a A₁•T₂₇ and G₇•C₃₃ are either not hydrogen bonded or are in fast exchange with solvent, and, therefore, the imino proton signals are not observed.

similar to I ($\Delta\delta < 0.05$ ppm) with the exception of the resonances near the cross-link, which display the greatest deviation from I ($\Delta\delta = 0.09$ and 0.07 ppm for Y₈-A₁₃ and T₃₂-A₆, respectively). These deviations can be explained if either the cross-link introduces subtle changes in the electronic environment due to differences in ring current effects or by the presence of highly localized conformational changes caused by the linker. However, the fact that hydrogen bonding is observed for Y₈-A₁₃ on IV (and for V) suggests that the cross-link does not grossly alter the native structure and argues for the former alternative.

Similar to IV, the imino proton resonances near the cross-link for V display the largest change in chemical shift relative to I ($\Delta\delta = 0.33$ and 0.11 ppm for Y₈-A₁₃ and T₃₂-A₆, respectively; Figure 5). In addition, the resonances at A₅-T₁₆ and T₃₁-A₆ show a greater deviation in chemical shift relative to I than for sequence IV ($\Delta\delta = 0.14$ and 0.09 ppm for A₅-T₁₆ and T₃₁-A₆, respectively, in V, vs 0.03 ppm for the corresponding resonances in IV). Taken together, these subtle spectral differences between IV and V may indicate that the longer linker may be more structurally perturbing. However, the chemical shift values of the remaining imino protons in V are very similar to I ($\Delta\delta < 0.05$ ppm) suggesting that any conformational changes are highly localized.

The spectral changes that occur upon titrating I, IV, and V from pH 6.0 to 8.0 are presented in Figure 6. Upon raising the pH of I to 7.4, the imino proton resonances of G₇, T₈, and T₃₂ begin to shift and at pH 8.0 resonate at a new frequency (Figure 6a). The observation that a second set of narrow resonances appear at higher pH is consistent with an equilibrium between the hairpin and triplex forms of I.^{18d,39} By contrast, the ¹H NMR spectrum of IV remains unchanged over this entire pH range, which indicates that the hairpin form of IV does not exist under these solution conditions (Figure 6b).⁴² Moreover, at pH 8.0 there is no evidence of end-fraying near the cross-link as evidenced by the strong G₇, T₈, and T₃₂ imino proton signals. Titrating V from pH 6.0 to 8.0 does not appear to denature this triplex either; however, some of the resonances proximal to the cross-link broaden and shift, indicating that the triplex begins to fray at higher pH (Figure 6c). Although this observation can be explained if the cross-link introduces strain into the helix, this pattern of broadening is similar to that observed for I and therefore suggests that the longer linker possibly allows for

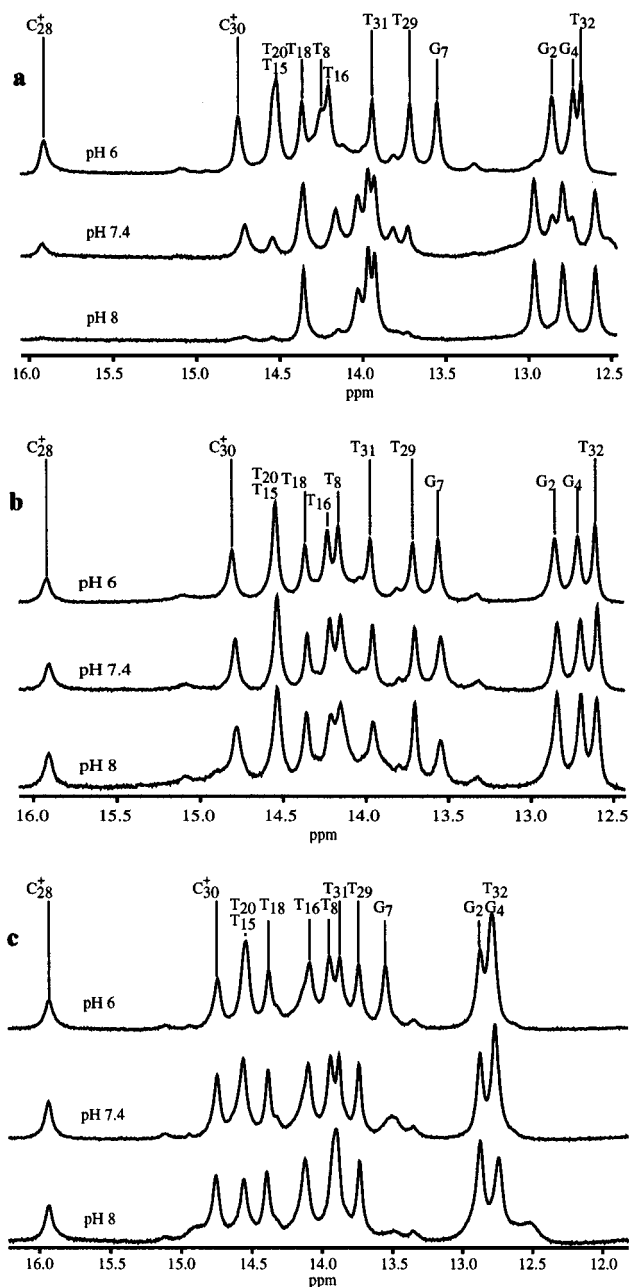


Figure 6. 500 MHz ¹H NMR spectra of the imino proton region of I, IV, and V (a, b, and c, respectively) as a function of pH at 1 °C in PBS buffer (90% H₂O/10% D₂O) with MgCl₂ (0.5 mM).

“breathing” at the triplex terminus.⁴³ Significantly, titrating each sequence back to the starting pH value affords spectra that are identical with the original spectra measured at pH 6 and is consistent with the results obtained by CD spectroscopy.

NMR melting studies of I and IV were performed at pH 6.0, 7.4, and 8.0 to examine the denaturation pathway of these structures.⁴⁴ Upon heating I at pH 6.0, the terminal Watson-Crick base-pairs and the rapidly exchanging protonated cytosine residues begin to fray prior to 50 °C.³⁵ This fraying is followed by a sharp melting of the remaining imino proton resonances when the temperature is increased to 60 °C. The absence of any additional imino protons upon the thermal denaturation of I indicates that, at least on the NMR time scale, this sequence melts from the triplex to a single-stranded oligomer without

(43) Putnam, B. F.; van Zandt, L. L.; Prohofsky, E. W.; Mei, W. N. *Biophys. J.* **1981**, *35*, 271–287 and references therein.

(44) Lefevre, J.-F.; Lane, A. N.; Jardetzky, O. *J. Mol. Biol.* **1985**, *185*, 689–699.

(42) This finding is supported by DSC data under similar solution conditions.¹⁷

forming intermediate structures, a result consistent with UV and DSC measurements of this sequence.¹⁷ The imino proton melting spectrum of IV at pH 6.0 is very similar to I.³⁵ Specifically, the terminal Watson-Crick base-pairs and the rapidly exchanging protonated cytosine residues fray prior to complete melting of the triplex. In contrast to I, significant hydrogen bonding exists in IV at 60 °C as evident by the strong imino resonances. The fact that the chemical shift differences between I and IV are nearly identical as the temperature is increased suggests that although the cross-link provides an increase in thermal stability, the length, composition, and location of the cross-link do not alter the thermal denaturation pathway.

Several broad imino resonances corresponding to both the triplex and hairpin are present in the spectrum of I at 1 °C and pH 7.4.³⁵ Heating to 20 °C shifts the equilibrium between these structures in favor of the hairpin. As I is further heated to 50 °C, the hairpin resonances eventually broaden into the baseline. This thermal transition from triplex to single-strand coincides well with the melting temperatures of I as determined by UV and DSC experiments.³⁸ By contrast, the temperature-dependent imino proton spectra of IV at pH 7.4 shows that, although the terminal Watson-Crick base-pairs and the rapidly exchanging protonated cytosine residues begin to fray prior to 50 °C, the triplex remains intact up to 50 °C without the presence of any hairpin structure.³⁵ Significantly, with the exception of the lower melting temperatures, this imino proton melting spectrum of IV at pH 7.4 (and pH 8.0) remains very similar to the melting spectrum of I at pH 6.0.

Discussion

Triple helices containing cytosine residues in the Hoogsteen strand form under very specific solution conditions, typically below pH 7.³ In addition to limiting their utility *in vitro* and perhaps *in vivo*, this pH dependence has hampered progress in determining the structural and thermodynamic properties of third strand binding at physiological pH.⁴⁵ The availability of a conformationally stable, homogeneous model triplex for detailed biophysical characterization would significantly advance these studies. For example, a conformationally stable model system should allow for crystallographic study of a complete helical turn of a triple helix,⁴⁶ as well as a further assessment of the effects of multiple base-triplet mismatches, bulges, or stretches of contiguous C⁺ residues in the Hoogsteen strand.⁴⁷

We have designed, synthesized, and characterized stable triplex structures by covalently attaching the third strand to a Watson-Crick duplex through a disulfide cross-link. Formation of the disulfide bond in IV results in an increase in the apparent

pK_a up to 1.5 units resulting in a triplex that is structurally homogeneous at pH 7.4 and at 37 °C, and up to pH 8.0 at 25 °C. CD, NMR, and UV measurements suggest that the cross-link does not appear to perturb native helical geometry. Although we have not performed full structural determinations for I–V, the spectral observations reported here are consistent with those for other disulfide cross-linked oligonucleotides previously determined to be isomorphous with their wild-type sequences.⁴⁸

A variety of other techniques are available to stabilize third strand binding in pyr·pur–pyr triplexes containing C⁺·G–C base-triplets.^{5,7} One general method stabilizes third strand binding through noncovalent interactions between the DNA and intercalators,⁴⁹ minor groove binders,⁵⁰ or polyamines.⁵¹ The benzopyridindoles,^{8c,49b} which intercalate in stretches of T·A–T triplets, afford the greatest thermal stabilization, with ΔT_m values up to +31 °C (the effect such compounds have on the apparent pK_a of cytosine have not been addressed). A second family of methods centers on chemical modification of the Hoogsteen cytosine residues.^{3,6,52} For example, alkylation of the C⁵-position can provide an increase in the apparent pK_a of the N³-proton by as much as 1.0 unit.^{6f,18a} Alternatively, removing the requirement for N³-protonation entirely by the *de novo* design of bases that mimic the protonated edge of cytosine can result in triplex binding that is no longer pH dependent.^{6b,j,52a,b}

While both types of methods are useful in stabilizing triple helices for studies *in vivo*, their utility for constructing model triplexes to examine the structural and thermodynamic aspects of triplex formation *in vitro* is less useful. For example, one drawback in the use of intercalators both *in vitro* and *in vivo* is that specific recognition sequences must be present for binding to occur^{5,49b} and this sequence dependence ultimately limits the types of triplexes that can be investigated. Furthermore, intercalators and some base modifications can significantly alter the backbone geometry near the sites of modification; such perturbations may be undesirable if these constructs are being

(45) For representative structural studies, see: ref 1a and (a) Macaya, R.; Wang, E.; Schultze, P.; Sklenář, V.; Feigon, J. *J. Mol. Biol.* **1992**, *225*, 755–773. For examples of the thermodynamic properties of triplexes, see: (b) Cheng, Y.-K.; Pettitt, B. M. *Prog. Biophys. Mol. Biol.* **1992**, *58*, 225–257. (c) Plum, G. E.; Park, Y.-W.; Singleton, S. F.; Dervan, P. B.; Breslauer, K. J. *Proc. Natl. Acad. Sci. U.S.A.* **1990**, *87*, 9436–9440.

(46) The crystal structure of a two-base pur·pur–pyr triplex has been reported; see: van Meervelt, L.; Vlieghe, D.; Dautant, A.; Gallois, B.; Précigoux, G.; Kennard, O. *Nature* **1995**, *374*, 742–744.

(47) (a) Wang, Y.; Patel, D. J. *Biochemistry* **1995**, *34*, 5696–5704. (b) Best, G. C.; Dervan, P. B. *J. Am. Chem. Soc.* **1995**, *117*, 1187–1193. (c) Fossella, J. A.; Kim, Y. V.; Shih, H.; Richards, E. G.; Fresco, J. R. *Nucleic Acids Res.* **1993**, *21*, 4511–4515. (d) Rougée, M.; Faucon, B.; Mergny, J. L.; Barcelo, F.; Giovannangeli, C.; Garestier, T.; Hélène, C. *Biochemistry* **1992**, *31*, 9269–9278. (e) Beal, P. A.; Dervan, P. B. *Nucleic Acids Res.* **1992**, *20*, 2773–2776. (f) Sun, J.-S.; Mergny, J.-L.; Lavery, R.; Montenay-Garestier, T.; Hélène, C. *J. Biomol. Struct. Dyn.* **1991**, *9*, 411–424. (g) Macaya, R. F.; Gilbert, D. E.; Malek, S.; Sinsheimer, J. S.; Feigon, J. *Science* **1991**, *254*, 270–274. (h) Roberts, R. W.; Crothers, D. M. *Proc. Natl. Acad. Sci. U.S.A.* **1991**, *88*, 9397–9401. (i) Brown, T.; Leonard, G. A.; Booth, E. D.; Kneale, G. J. *J. Mol. Biol.* **1990**, *212*, 437–440.

(48) (a) Cain, R. J.; Zuiderweg, E. R. P.; Glick, G. D. *Nucleic Acids Res.* **1995**, *23*, 2153–2160. (b) Wang, H.; Zuiderweg, E. R. P.; Glick, G. D. *J. Am. Chem. Soc.* **1995**, *117*, 2981–2991. (c) Wang, H.; Osborne, S. E.; Zuiderweg, E. R. P.; Glick, G. D. *J. Am. Chem. Soc.* **1994**, *116*, 5021–5022.

(49) (a) Marchand, C.; Bailly, C.; Nguyen, C. H.; Bisagni, E.; Garestier, T.; Hélène, C.; Waring, M. J. *Biochemistry* **1996**, *35*, 5022–5032. (b) Escudé, C.; Nguyen, C. H.; Mergny, J.-L.; Sun, J.-S.; Bisagni, E.; Garestier, T.; Hélène, C. *J. Am. Chem. Soc.* **1995**, *117*, 10212–10219. (c) Wilson, W. D.; Mizan, S.; Tanius, F. A.; Yao, S.; Zon, G. J. *Molec. Recog.* **1994**, *7*, 89–98. (d) Grigoriev, M.; Praseuth, D.; Robin, P.; Hemar, A.; Saison-Behmoaras, T.; Dautry-Varsat, A.; Thuong, N. T.; Hélène, C.; Harel-Bellan, A. *J. Biol. Chem.* **1992**, *267*, 3389–3395. (e) Giovannangeli, C.; Montenay-Garestier, T.; Rougée, M.; Chassignol, M.; Thuong, N. T.; Hélène, C. *J. Am. Chem. Soc.* **1991**, *113*, 7775–7777. (f) Sun, J.-S.; Giovannangeli, C.; François, J. C.; Kurfurst, R.; Montenay-Garestier, T.; Asseline, U.; Saison-Behmoaras, T.; Thuong, N. T.; Hélène, C. *Proc. Natl. Acad. Sci. U.S.A.* **1991**, *88*, 6023–6027.

(50) (a) Park, Y.-W.; Breslauer, K. J. *Proc. Natl. Acad. Sci. U.S.A.* **1992**, *89*, 6653–6657. (b) Durand, M.; Thuong, N. T.; Maurizot, J. C. *J. Biol. Chem.* **1992**, *267*, 24394–24399. (c) Mergny, J.-L.; Collier, D.; Rougée, M.; Montenay-Garestier, T.; Hélène, C. *Nucleic Acids Res.* **1991**, *19*, 1521–1526.

(51) (a) Pallan, P. S.; Ganesh, K. N. *Biochem. Biophys. Res. Commun.* **1996**, *222*, 416–420. (b) Barawkar, D. A.; Kumar, V. A.; Ganesh, K. N. *Biochem. Biophys. Res. Commun.* **1994**, *205*, 1665–1670. (c) Tung, C.-H.; Breslauer, K. J.; Stein, S. *Nucleic Acids Res.* **1993**, *21*, 5489–5494. (d) Thomas, T.; Thomas, T. J. *Biochemistry* **1993**, *32*, 14068–14074. (e) Hampel, K. J.; Crosson, P.; Lee, J. S. *Biochemistry* **1991**, *30*, 4455–4459.

(52) (a) Priestley, E. S.; Dervan, P. B. *J. Am. Chem. Soc.* **1995**, *117*, 4761–4765. (b) von Krosigk, U.; Benner, S. A. *J. Am. Chem. Soc.* **1995**, *117*, 5361–5362. (c) Froehler, B. C.; Wadwani, S.; Terhorst, T. J.; Gerrard, S. R. *Tetrahedron Lett.* **1992**, *33*, 5307–5310. (d) Froehler, B. C.; Ricca, D. J. *J. Am. Chem. Soc.* **1992**, *114*, 8320–8322. (e) Miller, P. S.; Bhan, P.; Cushman, C. D.; Trapane, T. L. *Biochemistry* **1992**, *31*, 6788–6793.

used to study the intrinsic conformational and thermodynamic features of triplex DNA.^{5,53}

To our knowledge, the largest difference in both thermal and pH stability between a native and modified triplex occurs with the disulfide cross-linked triplex IV. As discussed elsewhere, cross-link formation leads to two-state melting and an increase in thermal stability that is due solely to entropic effects (i.e., the cross-link is enthalpically neutral).^{13,17} Moreover, covalently restraining the Hoogsteen strand within the major groove results in conformationally homogeneous triplex structures in which the ΔT_m is independent of $[Mg^{2+}]$. These results are particularly striking given that IV contains a high percentage of C⁺·G–C base-triplets relative to the other sequences studied previously.⁵⁴ In principle, our chemistry can be used to stabilize other triplex structures because the cross-link can be incorporated site-specifically and in a sequence independent manner. Furthermore, the type of triplex structure to be constrained is not limited to just intramolecular triplexes, since intermolecular structures simply would require cross-links at both termini (e.g., see Figure 1).

To summarize, we have described the design and synthesis of two intramolecular pyr·pur–pyr triple helices containing disulfide cross-links. CD and NMR measurements indicate that the cross-link does not significantly perturb the geometry of IV and V relative to their unmodified counterpart. These cross-links extend the thermal and pH stability of triple helices so that these unique nucleic acid structures can be studied under a wide range of solution conditions. Furthermore, because the cross-link effectively prevents conformational heterogeneity associated with pyr·pur–pyr triple helices containing C⁺·G–C base-triplets under physiologically relevant conditions,^{18d,45a,55} these constructs should serve as effective model systems to aid in the development of sequences that bind with higher affinity and specificity.

Experimental Section

Monomer Synthesis. Reagents were purchased from Aldrich Chemical Co. (Milwaukee, WI). CH₃CN, CH₂Cl₂, *N,N*-diisopropylethylamine, pyridine, and Et₃N were each distilled from CaH₂ under an N₂ atmosphere. MeOH was dried by distillation from magnesium methoxide. DMF was dried by storing for 1 week over activated 4 Å molecular sieves and then decanting onto fresh sieves prior to use. Silica gel (32–63 mesh) for flash chromatography was obtained from ICN Biochemicals (Cleveland, OH). Glass-backed plates for thin-layer chromatography precoated with a 0.25-mm-thick layer of Kieselgel 60F-254 was obtained from E. Merck (Darmstadt, Germany). Spots were visualized by UV quenching (254 nm) or by staining the plate in ceric ammonium molybdate (48.0 g of ammonium molybdate and 2.0 g of cerium(II)sulfate in 1 L of 10% aqueous sulfuric acid). ¹H and ¹³C NMR spectra were measured on either a Bruker AM 360 MHz or an AM 300 MHz spectrometer and ³¹P NMR spectra on a Bruker AMX 500 spectrometer at 202 MHz. All NMR spectra were measured at ambient probe temperature using either CHCl₃ ($\delta = 7.26$), CD₂HOD ($\delta = 3.40$), or CD₂HCN ($\delta = 1.93$) as an internal reference except for ³¹P NMR which is referred to trimethyl phosphate ($\delta = 0.00$). Infrared spectra were measured on a Nicolet Model 5D Fourier-transform spectrophotometer. Bands are reported in reciprocal centimeters (cm⁻¹) and were calibrated by comparison with the 1601 cm⁻¹ stretch in polystyrene. Mass spectra were measured by either fast atom bombardment (FAB) on a VG Instruments Model 7070 spectrometer with 3-nitrobenzyl alcohol (3-NBA) as a matrix or direct chemical ionization

(DCI) with either methane (CH₄) or ammonia (NH₄⁺) as matrices. Yields refer to chromatographically and spectroscopically homogeneous materials.

C⁵-(Allyl)-2'-deoxyuridine (1).²² PdCl₂ (0.63 g, 3.56 mmol, 0.25 equiv) and LiCl₂ (0.30 g, 7.13 mmol, 0.5 equiv) were suspended in MeOH (35 mL). This solution was sparged with N₂ for 15 min and then added to C⁵-chloromercuri-2'-deoxyuridine²³ (6.60 g, 14.25 mmol) and allyl chloride (11.6 mL, 142.5 mmol, 10 equiv) dissolved in MeOH (150 mL). The reaction mixture was stirred under N₂ for 20 h and then quenched by bubbling H₂S for 2 min. The solution was filtered through Celite, concentrated under reduced pressure, and chromatographed on silica gel (eluting with 10% MeOH in CH₂Cl₂) to afford **1** (3.45 g, 78% yield) as a colorless, opaque glass. TLC (9:1 CH₂Cl₂/MeOH) *R*_f = 0.33. ¹H NMR (360 MHz, CD₃OD) δ 2.26–2.40 (2 H, m, 2'-H_{a,b}), 3.13 (2 H, dd, *J* = 1.2, 6.5 Hz, 7-H_{a,b}), 3.81 (1 H, dd, *J* = 3.6, 12.0 Hz, 5'-H_a), 3.88 (1 H, dd, *J* = 3.2, 12.0 Hz, 5'-H_b), 4.01 (1 H, dd, *J* = 3.4, 6.7 Hz, 4'-H), 4.47–4.50 (1 H, m, 3'-H), 5.13–5.23 (2 H, m, 9-H) (*cis* and *trans*), 5.93–6.04 (1 H, m, 8-H), 6.31 (1 H, t, *J* = 6.7 Hz, 1'-H), 7.89 (1 H, s, 6-H). ¹³C NMR (90 MHz, CD₃OD) δ 31.8 (7), 41.4 (2'), 62.9 (5'), 72.3 (3'), 86.6 (1'), 89.0 (4'), 114.3 (5), 117.2 (9), 136.3 (6), 138.9 (8), 152.3 (2), 165.8 (4). IR (film; NaCl) ν 3394, 1689, 1471, 1275, 1093, 1054 cm⁻¹. DCI MS (NH₄⁺) *m/z* 269 (M⁺ + 1).

3',5'-Bis-*O*-(*tert*-butyldimethylsilyl)-C⁵-(allyl)-2'-deoxyuridine (2). Imidazole (2.65 g, 39.0 mmol, 4.4 equiv) and **1** (2.38 g, 8.87 mmol) were dissolved in DMF (20 mL), and *tert*-butyldimethylsilyl chloride (2.94 g, 19.5 mmol, 2.2 equiv) was added. The reaction mixture was stirred under N₂ for 3 h after which the solution was diluted with EtOAc and washed with saturated NaHCO₃ and brine. The organic layer was dried over Na₂SO₄ and concentrated under reduced pressure to give a white solid. The residue was chromatographed on silica gel (eluting with 40% EtOAc in petroleum ether) to afford **2** (3.45 g, 78% yield) as a colorless glass. TLC (1:1 EtOAc/petroleum ether) *R*_f = 0.73. ¹H NMR (360 MHz, CDCl₃) δ 0.07, 0.07, 0.09 (12 H, 3 s, 2 (CH₃)₂Si), 0.88, 0.91 (18 H, 2 s, 2 (CH₃)₃CSi), 2.00 (1 H, dd, *J* = 5.7, 7.7 Hz, 2'-H_a), 2.24 (1 H, dd, *J* = 2.5, 5.7 Hz, 2'-H_b), 3.06 (2 H, dd, *J* = 1.0, 6.4 Hz, 7-H_{a,b}), 3.72–3.81 (2 H, m, 5'-H_{a,b}), 3.92 (1 H, d, *J* = 10.2 Hz, 4'-H), 4.38–4.39 (1 H, m, 3'-H), 5.05–5.12 (2 H, m, 9-H) (*cis* and *trans*), 5.82–5.89 (1 H, m, 8-H), 6.31 (1 H, dd, *J* = 5.8, 8.0 Hz, 1'-H), 7.36 (1 H, s, 6-H), 9.10 (1 H, s, NH). ¹³C NMR (90 MHz, CDCl₃) δ -5.5, -5.4, -4.9, -4.7 ((CH₃)₂Si), 18.0, 18.4 ((CH₃)₃CSi), 25.7, 25.9 ((CH₃)₃CSi), 30.8 (7), 41.1 (2'), 63.0 (5'), 72.2 (3'), 85.0 (1'), 87.8 (4'), 113.2 (5), 116.7 (9), 134.7 (6), 136.0 (8), 150.2 (2), 163.1 (4). IR (film; NaCl) ν 3189, 3060, 2955, 2892, 2858, 1715, 1685, 1471, 1405, 1274, 1097, 971 cm⁻¹. DCI MS (CH₄) *m/z* 497 (M⁺ + 1).

3',5'-Bis-*O*-(*tert*-butyldimethylsilyl)-C⁵-(2,3-dihydroxypropyl)-2'-deoxyuridine (3). Compound **2** (3.68 g, 7.41 mmol) and *N*-methylmorpholine *N*-oxide (0.95 g, 8.14 mmol, 1.1 equiv) were dissolved in acetone/H₂O (6:1, 105 mL), and OsO₄ (20 mg, 70 μ mol, 0.01 equiv) was added. The reaction mixture was stirred in the dark for 3 h after which an aqueous solution of saturated NaHSO₃ (1 mL) was added to precipitate osmium salts. The solution was decanted and the light brown residue was washed with Et₂O. The combined organic layers were dried over Na₂SO₄ and concentrated under reduced pressure to give an oily yellow solid. The residue was chromatographed on silica gel (eluting with a step gradient of 40–60% EtOAc in petroleum ether) to afford **3** (3.21 g, 82% yield) as a white tacky solid. TLC (1:1 EtOAc/petroleum ether) *R*_f = 0.09. ¹H NMR (360 MHz, CDCl₃) δ (two diastereomers at C-8) 0.06, 0.07, 0.09 (12 H, 3 s, 2 (CH₃)₂Si), 0.88, 0.91, (18 H, 2 s, 2 (CH₃)₃CSi), 1.97–2.03 (1 H, m, 2'-H_a), 2.22–2.27 (1 H, m, 2'-H_b), 2.48–2.52 (2 H, m, 7-H_{a,b}), 3.44–3.48 (1 H, m, 9-H_a), 3.60 (1 H, dd, *J* = 2.2, 11.8 Hz, 9-H_b), 3.72–3.76 (2 H, m, 5'-H_{a,b}), 3.81 (1 H, s, 8-H), 3.92–3.94 (1 H, m, 4'-H), 4.37–4.39 (1 H, m, 3'-H), 6.26–6.32 (1 H, m, 1'-H), 7.52, 7.55 (1 H, 2 s, 6-H). ¹³C NMR (90 MHz, CDCl₃) δ (two diastereomers at C-8) -5.4, -5.4, -4.9, -4.7 ((CH₃)₂Si) 18.0, 18.4 ((CH₃)₃CSi), 25.7, 25.9 ((CH₃)₃CSi), 31.4, 31.5 (7), 41.2, 41.3 (2'), 63.0 (5'), 65.7 (9), 71.3, 71.4 (8), 72.3 (3'), 85.0, 85.2 (1'), 87.9, 88.0 (4'), 111.1, 111.2 (5), 138.1 (6), 150.0 (2), 165.2 (4). IR (film; NaCl) ν 3447, 3397, 2954, 2896, 1716, 1684, 1472, 1291, 1255, 1094, 1027, 834, 778, 668, 612 cm⁻¹.

(53) Collier, D. A.; Mergny, J.-L.; Thuong, N. T.; Hélène, C. *Nucleic Acids Res.* **1991**, *19*, 4219–4224.

(54) Most sequences that contain >30% C⁺·G–C base-triplets have 5-methyl-2'-deoxycytidine in place of 2'-deoxycytidine.^{8e,49d,51c,52a,c,d}

(55) Radhakrishnan, I.; de los Santos, C.; Patel, D. J. *J. Mol. Biol.* **1991**, *221*, 1403–1418.

3',5'-Bis-*O*-(*tert*-butyldimethylsilyl)-*C*⁵-(ethanal)-2'-deoxyuridine (4). Compound **3** (3.21 g, 6.05 mmol) was dissolved in *p*-dioxane/H₂O (3:1, 60 mL), and NaO₄ (1.55 g, 7.26 mmol, 1.2 equiv) was added. The reaction mixture was stirred for 3 h and diluted with Et₂O to precipitate the inorganic salts. The organic layer was decanted and washed with water. The organic extract was dried with Na₂SO₄, concentrated under reduced pressure, and chromatographed on silica gel (eluting with a step gradient of 40–60% Et₂O in petroleum ether) to afford **4** (2.94 g, 97% yield) as a colorless viscous oil. TLC (2:3 EtOAc/petroleum ether) *R*_f = 0.52. ¹H NMR (360 MHz, CDCl₃) δ 0.07, 0.08, 0.08 (12 H, 3 s, 2 (CH₃)₂Si), 0.89, 0.90 (18 H, 2 s, 2 (CH₃)₃-CSi), 2.02 (1 H, ddd, *J* = 6.7, 7.0, 13.4 Hz, 2'-H_a), 2.29 (1 H, dd, *J* = 2.5, 7.5 Hz, 2'-H_b), 3.32–3.47 (2 H, m, 7-H_{a,b}), 3.82–3.86 (2 H, m, 5'-H_{a,b}), 3.94 (1 H, br s, 4'-H), 4.38–4.39 (1 H, m, 3'-H), 6.31 (1 H, t, *J* = 6.7 Hz, 1'-H), 7.61 (1 H, s, 6-H), 8.93 (1 H, s, NH), 9.70 (1 H, s, 8-H). ¹³C NMR (90 MHz, CDCl₃) δ -5.4, -5.4, -4.9, -4.7 ((CH₃)₂-Si), 18.0, 18.4 ((CH₃)₃CSi), 25.7, 25.9 ((CH₃)₃CSi), 41.0 (2'), 41.6 (7), 63.0 (5'), 72.2 (3'), 85.3 (1'), 88.0 (4'), 106.6 (5), 138.5 (6), 149.9 (2), 162.9 (4), 197.0 (8). IR (film; NaCl) ν 3232, 2901, 2850, 1733, 1472, 1275, 1106, 1030, 835, 778 cm⁻¹.

3',5'-Bis-*O*-(*tert*-butyldimethylsilyl)-*C*⁵-(iodo)-2'-deoxyuridine (5).²⁵ 5-Iodo-2'-deoxyuridine (1.89 g, 5.34 mmol) was dissolved in DMF (21.4 mL), and imidazole (1.60 g, 23.50 mmol, 4.4 equiv) and *tert*-butyldimethylsilyl chloride (1.77 g, 11.75 mmol, 2.2 equiv) were added. The reaction mixture was stirred under N₂ and, after 2 h, the solution was diluted with Et₂O and washed with saturated NaHCO₃ and brine. The organic extract was dried over Na₂SO₄ and concentrated under reduced pressure to give an oily solid. The residue was chromatographed on silica gel (eluting with 2:1 petroleum ether/EtOAc) to afford **5** (2.85 g, 92% yield) as a white foam. TLC (2:1 petroleum ether/EtOAc) *R*_f = 0.29. ¹H NMR (360 MHz, CDCl₃) δ 0.07, 0.08, 0.15, 0.16 (12 H, 4 s, 2 (CH₃)₂Si), 0.88, 0.91 (18 H, 2 s, 2 (CH₃)₃CSi), 1.99 (1 H, ddd, *J* = 5.9, 8.1, 13.3 Hz, 2'-H_a), 2.30 (1 H, ddd, *J* = 2.2, 5.6, 13.3 Hz, 2'-H_b), 2.48–2.52 (2 H, m, 7-H_{a,b}), 3.44–3.48 (1 H, m, 9-H_a), 3.60 (1 H, dd, *J* = 2.2, 11.8 Hz, 9-H_b), 3.76 (1 H, dd, *J* = 2.3, 11.5 Hz, 5'-H_a), 3.89 (1 H, dd, *J* = 2.3, 11.5 Hz, 5'-H_b), 3.99 (1 H, d, *J* = 2.3 Hz, 4'-H), 4.38–4.40 (1 H, m, 3'-H), 6.27 (1 H, dd, *J* = 5.6, 8.1 Hz, 1'-H), 8.09 (1 H, s, 6-H), 8.55 (1 H, br s, NH). ¹³C NMR (90 MHz, CDCl₃) δ -5.3, -5.1, -4.9, -4.7 ((CH₃)₂Si), 18.0, 18.5 ((CH₃)₃CSi), 25.7, 26.2 ((CH₃)₃CSi), 42.0 (2'), 63.1 (5'), 68.2 (5), 72.6 (3'), 85.8 (1'), 88.5 (4'), 144.4 (6), 149.7 (2), 159.8 (4). IR (film; NaCl) ν 2954, 2929, 2857, 1703, 1690, 1274, 1255, 836, 778 cm⁻¹. FAB MS (3-NBA) *m/z* 583 (M⁺ + 1).

3',5'-Bis-*O*-(*tert*-butyldimethylsilyl)-*C*⁵-(4-hydroxy-1-butylnyl)-2'-deoxyuridine (6).²⁶ Compound **5** (1.98 g, 3.08 mmol) was dissolved in DMF (12 mL) and the mixture was degassed under reduced pressure for 5 min. Et₃N (0.9 mL, 6.17 mmol, 2.0 equiv), but-3-yn-1-ol (0.7 mL, 9.25 mmol, 3.0 equiv), CuI (0.18 g, 0.62 mmol, 0.2 equiv), and (Ph₃P)₄Pd (0.36 g, 0.31 mmol, 0.1 equiv) were added. The reaction mixture was stirred under N₂ for 18 h after which the solution was diluted with EtOAc and washed with saturated NaHCO₃ and brine. The organic layer was dried over Na₂SO₄ and concentrated under reduced pressure to give a brown oil. The residue was chromatographed on silica gel (eluting with a step gradient of 40–60% EtOAc in petroleum ether) to afford **6** (1.29 g, 79% yield) as a white foam. TLC (1:1 EtOAc/petroleum ether) *R*_f = 0.36. ¹H NMR (360 MHz, CDCl₃) δ 0.07, 0.08, 0.13, 0.14 (12 H, 4 s, 2 (CH₃)₂Si), 0.89, 0.93 (18 H, 2 s, 2 (CH₃)₃CSi), 2.02 (1 H, ddd, *J* = 5.8, 7.5, 13.2 Hz, 2'-H_a), 2.19 (1 H, br s, 10-OH), 2.30 (1 H, ddd, *J* = 2.7, 5.9, 13.2 Hz, 2'-H_b), 2.65 (2 H, t, *J* = 6.3 Hz, 9-H_{a,b}), 3.76 (1 H, dd, *J* = 2.1, 11.4 Hz, 5'-H_a), 3.78 (2 H, t, *J* = 6.3 Hz, 10-H_{a,b}), 3.90 (1 H, dd, *J* = 2.3, 11.4 Hz, 5'-H_b), 3.97 (1 H, dd, *J* = 5.9, 7.5 Hz, 1'-H), 7.96 (1 H, s, 6-H), 8.46 (1 H, br s, NH). ¹³C NMR (90 MHz, CDCl₃) δ -5.6, -5.4, -4.9, -4.7 ((CH₃)₂-Si), 18.0, 18.4 ((CH₃)₃CSi), 24.0 (9), 25.7, 26.0 ((CH₃)₃CSi), 42.0 (2'), 60.8 (5'), 62.9 (10), 72.3 (3'), 73.4 (8), 85.7 (1'), 88.3 (4'), 91.7 (7), 100.2 (5), 141.9 (6), 149.0 (2), 161.7 (4). IR (KBr) ν 3416, 2954, 2930, 2857, 2242, 1725, 1683, 1471, 1255, 1097, 835 cm⁻¹. DCI MS (isobutane) *m/z* 525 (M⁺ + 1).

3',5'-Bis-*O*-(*tert*-butyldimethylsilyl)-*C*⁵-(2-hydroxyethyl)-2'-deoxyuridine (7a). Compound **4** (2.94 g, 5.89 mmol) was dissolved in MeOH (50 mL), and NaBH₄ (58 mg, 1.53 mmol, 0.26 equiv) was added. The reaction mixture was stirred for 3 h after which the reaction was

diluted with Et₂O and washed with saturated NaHCO₃ and brine. The aqueous layer was washed once with Et₂O, and the combined organic layers were dried with Na₂SO₄, concentrated under reduced pressure, and chromatographed on silica gel (eluting with a step gradient of 25–50% EtOAc in petroleum ether) to afford **7a** (2.00 g, 68% yield) as a white solid. TLC (2:3 EtOAc/petroleum ether) *R*_f = 0.37. ¹H NMR (360 MHz, CD₃CN) δ 0.09 (12 H, s, 2 (CH₃)₂Si), 0.89, 0.91 (18 H, 2 s, 2 (CH₃)₃CSi), 2.08–2.14 (2 H, m, 2'-H_{a,b}), 2.43 (1 H, t, *J* = 6.3 Hz, 7-H_a), 2.87 (1 H, t, *J* = 5.8 Hz, 7-H_b), 3.54 (2 H, dd, *J* = 6.2, 12.2 Hz, 5'-H_{a,b}), 3.75 (2 H, d, *J* = 3.8 Hz, 8-H_{a,b}), 3.86 (1 H, dd, *J* = 3.7, 6.6 Hz, 4'-H), 4.38–4.41 (1 H, m, 3'-H), 6.17 (1 H, dd, *J* = 6.2, 7.7 Hz, 1'-H), 7.39 (1 H, s, 6-H), 9.08 (1 H, br s, NH). ¹³C NMR (90 MHz, CD₃CN) δ -5.2, -4.6 ((CH₃)₂Si), 18.8, 19.0 ((CH₃)₃CSi), 26.1, 26.3 ((CH₃)₃CSi), 31.5 (7), 41.0 (2'), 61.3 (8), 64.1 (5'), 73.4 (3'), 85.4 (1'), 88.5 (4'), 112.5 (5), 138.0 (6), 149.9 (2), 162.9 (4). IR (film; NaCl) ν 3415, 3192, 3061, 2936, 1716, 1464, 1376, 1255, 1119, 1072, 967, 836, 777, 672 cm⁻¹. DCI MS (CH₄) *m/z* 501 (M⁺ + 1).

3',5'-Bis-*O*-(*tert*-butyldimethylsilyl)-*C*⁵-(4-hydroxybutyl)-2'-deoxyuridine (7b). Compound **6** (1.29 g, 2.46 mmol) was placed in a Parr bottle and dissolved in MeOH (50 mL); the solution was degassed under reduced pressure for 5 min. Pd (10% on activated carbon, 0.26 g, 0.12 mmol, 0.05 equiv) was added and the reaction vessel was pressurized with H₂ (35 psi). The reaction mixture was shaken at room temperature in the dark for 12 h and then filtered through Celite washing to remove the catalyst. The residue was concentrated under reduced pressure and chromatographed on silica gel (eluting with 1:1 EtOAc/petroleum ether) to afford **7b** (0.92 g, 71% yield) as a white solid. TLC (1:1 EtOAc/petroleum ether) *R*_f = 0.23. ¹H NMR (360 MHz, CDCl₃) δ 0.06, 0.07, 0.10, 0.10 (12 H, 4 s, 2 (CH₃)₂Si), 0.88, 0.91 (18 H, 2 s, 2 (CH₃)₃CSi), 1.55–1.63 (4 H, m, 8-H_{a,b}, 9-H_{a,b}), 1.99 (1 H, ddd, *J* = 6.0, 8.1, 13.1 Hz, 2'-H_a), 2.05 (1 H, br s, 10-OH), 2.24 (1 H, ddd, *J* = 2.4, 5.7, 13.1 Hz, 2'-H_b), 2.29–2.38 (2 H, m, 7-H_{a,b}), 3.65 (2 H, t, *J* = 6.1 Hz, 10-H_{a,b}), 3.74 (1 H, dd, *J* = 2.7, 11.4 Hz, 5'-H_a), 3.84 (1 H, dd, *J* = 2.8, 11.4 Hz, 5'-H_b), 3.92 (1 H, dd, *J* = 2.6, 5.3 Hz, 4'-H), 4.38 (1 H, ddd, *J* = 2.4, 5.3, 6.0 Hz, 3'-H), 6.31 (1 H, dd, *J* = 5.7, 8.1 Hz, 1'-H), 7.42 (1 H, s, 6-H), 9.10 (1 H, br s, NH). ¹³C NMR (90 MHz, CDCl₃) δ -5.5, -5.4, -4.9, -4.7 ((CH₃)₂Si), 18.0, 18.4 ((CH₃)₃CSi), 25.3 (8), 25.7, 25.9 ((CH₃)₃CSi), 26.9 (7), 32.1 (9), 41.2 (2'), 62.3 (5'), 63.0 (10), 72.2 (3'), 84.8 (1'), 87.8 (4'), 115.0 (5), 135.7 (6), 150.2 (2), 163.6 (4). IR (film; NaCl) ν 2930, 1689, 1686, 1471, 1256, 1102, 886 cm⁻¹. FAB MS (3-NBA) *m/z* 529 (M⁺ + 1).

3',5'-Bis-*O*-(*tert*-butyldimethylsilyl)-*C*⁵-(2-methanesulfonyl)-2'-deoxyuridine (8a). Compound **7a** (2.00 g, 4.00 mmol) was dissolved in CH₂Cl₂ (40 mL) and pyridine (3.23 mL, 40 mmol, 10 equiv) and the solution was cooled to 0 °C under a N₂ atmosphere. Methanesulfonyl chloride (0.37 mL, 4.80 mmol, 1.2 equiv) was added dropwise and the reaction was stirred while gradually warming to room temperature overnight. The reaction was diluted with Et₂O and washed with saturated NaHCO₃ and brine. The organic layer was dried over Na₂SO₄, concentrated under reduced pressure, and chromatographed on silica gel (eluting with a step gradient of 50–100% Et₂O in petroleum ether) to afford **8a** (2.04 g, 88% yield) as a white foam. TLC (1:1 EtOAc/petroleum ether) *R*_f = 0.54. ¹H NMR (360 MHz, CDCl₃) δ 0.07, 0.08, 0.10 (12 H, 3 s, 2 (CH₃)₂Si), 0.89, 0.92 (18 H, 2 s, 2 (CH₃)₃CSi), 2.01–2.05 (1 H, m, 2'-H_a), 2.25 (1 H, dd, *J* = 2.3, 7.5 Hz, 2'-H_b), 2.73–2.76 (2 H, m, 7-H_{a,b}), 2.97 (3 H, s, CH₃SO₂), 3.75 (1 H, dd, *J* = 2.9, 11.3 Hz, 5'-H_b), 3.83 (1 H, dd, *J* = 3.1, 11.3 Hz, 5'-H_a), 3.93–3.94 (1 H, m, 4'-H), 4.36–4.40 (2 H, m, 3'-H, 8-H_{a,b}), 6.31 (1 H, dd, *J* = 6.1, 7.5 Hz, 1'-H), 7.55 (1 H, s, 6-H). ¹³C NMR (90 MHz, CDCl₃) δ -5.5, -5.4, -4.9, -4.7 ((CH₃)₂Si), 17.9, 18.3 ((CH₃)₃CSi), 25.7, 25.9 ((CH₃)₃CSi), 27.9 (7), 37.4 (CH₃SO₂), 41.2 (2'), 63.0 (5'), 67.9 (8), 72.2 (3'), 85.0 (1'), 87.9 (4'), 109.0 (5), 138.3 (6), 150.0 (2), 163.2 (4). IR (film; NaCl) ν 3792, 2919, 1694, 1453, 1375, 1171, 965, 840, 723, 668 cm⁻¹. FAB MS (3-NBA) *m/z* 579 (M⁺ + 1).

3',5'-Bis-*O*-(*tert*-butyldimethylsilyl)-*C*⁵-(4-methanesulfonyl)-2'-deoxyuridine (8b). Compound **7b** (0.92 g, 1.74 mmol) was dissolved in CH₂Cl₂ (17 mL) and pyridine (1.4 mL, 17.36 mmol, 10 equiv) and was cooled to 0 °C under a N₂ atmosphere. Methanesulfonyl chloride (0.19 mL, 2.43 mmol, 1.4 equiv) was added dropwise over a period of 30 min. The mixture was stirred while gradually warming to room temperature overnight. The residue was concentrated under

reduced pressure and chromatographed on silica gel (eluting with 1:1 EtOAc/petroleum ether) to afford **8b** (0.97 g, 92% yield) as a white foam. TLC (1:1 EtOAc/petroleum ether) $R_f = 0.42$. $^1\text{H NMR}$ (360 MHz, CDCl_3) δ 0.07, 0.08, 0.09, 0.11 (12 H, 4 s, 2 (CH_3)₂Si), 0.89, 0.92 (18 H, 2 s, 2 (CH_3)₃CSi), 1.60–1.65 (2 H, m, 8- $H_{\text{a,b}}$), 1.73–1.79 (2 H, m, 9- $H_{\text{a,b}}$), 1.99 (1 H, ddd, $J = 6.0, 8.2, 13.0$ Hz, 2'- H_{a}), 2.25 (1 H, ddd, $J = 2.3, 5.6, 13.0$ Hz, 2'- H_{b}), 2.34 (2 H, dd, $J = 7.8, 15.8$ Hz, 7- $H_{\text{a,b}}$), 3.00 (3 H, s, CH_3SO_2), 3.76 (1 H, dd, $J = 2.7, 11.4$ Hz, 5'- H_{a}), 3.85 (1 H, dd, $J = 2.8, 11.4$ Hz, 5'- H_{b}), 3.94 (1 H, dd, $J = 2.6, 5.1$ Hz, 4'- H), 4.20 (2 H, t, $J = 6.4$ Hz, 10- $H_{\text{a,b}}$), 4.39 (1 H, ddd, $J = 2.3, 5.1, 6.0$ Hz, 3'- H), 6.31 (1 H, dd, $J = 5.6, 8.2$ Hz, 1'- H), 7.45 (1 H, s, 6- H), 8.50 (1 H, br s, NH). $^{13}\text{C NMR}$ (90 MHz, CDCl_3) δ -5.4, -5.4, -4.8, -4.7 ((CH_3)₂Si), 17.9, 18.4 ((CH_3)₃CSi), 25.2 (8), 25.7, 25.9 ((CH_3)₃-CSi), 26.9 (7), 28.8 (9), 37.3 (CH_3SO_2), 41.3 (2'), 63.1 (5'), 69.6 (10), 72.3 (3'), 84.9 (1'), 87.9 (4'), 114.3 (5), 136.0 (6), 150.0 (2), 163.1 (4). IR (film; NaCl) ν 3230, 3195, 2936, 1699, 1684, 1472, 1347, 1173, 936 cm^{-1} . FAB MS (3-NBA) m/z 607 ($\text{M}^+ + 1$).

3',5'-Bis-*O*-(*tert*-butyldimethylsilyl)- C^5 -(thiobenzoyl)-2'-deoxyuridine (9a). Compound **8a** (2.04 g, 3.52 mmol) was dissolved in DMF (10 mL), and Et_3N (2.45 mL, 17.6 mmol, 5.0 equiv) and thiobenzoic acid (0.62 mL, 5.26 mmol, 1.5 equiv) were added. The reaction mixture was stirred under N_2 overnight, diluted with Et_2O , and washed with saturated NaHCO_3 and brine. The aqueous layer was washed once with Et_2O and the combined organic layers were dried over Na_2SO_4 , concentrated under reduced pressure, and chromatographed on silica gel (eluting with 25% EtOAc in petroleum ether) to afford **9a** (1.87 g, 86% yield) as a slightly orange-pink glass. TLC (3:7 EtOAc/petroleum ether) $R_f = 0.43$. $^1\text{H NMR}$ (300 MHz, CDCl_3) δ 0.05 (12 H, s, 2 (CH_3)₂Si), 0.88 (18 H, s, 2 (CH_3)₃CSi), 1.92 (1 H, ddd, $J = 6.0, 8.0, 13.1$ Hz, 2'- H_{a}), 2.17 (1 H, ddd, $J = 2.3, 5.8, 13.1$ Hz, 2'- H_{b}), 2.61–2.74 (2 H, m, 7- $H_{\text{a,b}}$), 3.27–3.32 (1 H, m, 8- H), 3.68–3.78 (2 H, m, 5'- $H_{\text{a,b}}$), 3.88–3.91 (1 H, m, 4'- H), 4.33–4.37 (1 H, m, 3'- H), 6.28 (1 H, dd, $J = 5.8, 8.0$ Hz, 1'- H), 7.44 (1 H, m, 6- H), 7.43–7.47 (2 H, m, ArH), 7.55–7.59 (1 H, m, ArH), 7.93–7.98 (2 H, m, ArH), 8.91 (1 H, br s, NH). $^{13}\text{C NMR}$ (90 MHz, CDCl_3) δ -5.6, -5.4, -4.9, -4.7 ((CH_3)₂Si), 17.9, 18.3 ((CH_3)₃CSi), 25.7, 25.8 ((CH_3)₃CSi), 27.7 (7), 28.0 (8), 41.0 (2'), 62.9 (5'), 72.2 (3'), 84.8 (1'), 87.7 (4'), 112.5 (5), 127.2, 128.5, 133.8, 136.7 (Ar), 136.9 (6), 150.2 (2), 163.3 (4), 191.5 (Ar). IR (film; NaCl) ν 3176, 3058, 2957, 2930, 2858, 1690, 1463, 1257, 1105, 1032, 839, 779, 673 cm^{-1} . DCI MS (CH_3) m/z 621 ($\text{M}^+ + 1$).

3',5'-Bis-*O*-(*tert*-butyldimethylsilyl)- C^5 -(thiobenzoyl)-2'-deoxyuridine (9b). Compound **8b** (0.95 g, 1.56 mmol) was dissolved in DMF (6.2 mL), and Et_3N (1.1 mL, 7.82 mmol, 5.0 equiv) and thiobenzoic acid (0.28 mL, 2.35 mmol, 1.5 equiv) were added. The reaction mixture was stirred under N_2 overnight. The reaction mixture was diluted with Et_2O and washed with saturated NaHCO_3 and brine. The organic layer was dried over Na_2SO_4 and concentrated under reduced pressure, and chromatographed on silica gel (eluting with 3:1 petroleum ether/EtOAc) to afford **9b** (0.93 g, 92% yield) as a slightly orange-pink foam. TLC (1:1 EtOAc/petroleum ether) $R_f = 0.58$. $^1\text{H NMR}$ (360 MHz, CDCl_3) δ 0.07, 0.07, 0.08, 0.09 (12 H, 4 s, 2 (CH_3)₂-Si), 0.89, 0.90 (18 H, 2 s, 2 (CH_3)₃CSi), 1.63–1.72 (4 H, m, 8- $H_{\text{a,b}}$, 9- $H_{\text{a,b}}$), 2.00 (1 H, ddd, $J = 6.0, 8.1, 13.1$ Hz, 2'- H_{a}), 2.23 (1 H, ddd, $J = 2.3, 5.7, 13.1$ Hz, 2'- H_{b}), 2.34 (2 H, t, $J = 7.1$ Hz, 7- $H_{\text{a,b}}$), 3.05–3.10 (2 H, m, 10- $H_{\text{a,b}}$), 3.75 (1 H, dd, $J = 2.8, 11.3$ Hz, 5'- H_{a}), 3.84 (1 H, dd, $J = 3.0, 11.3$ Hz, 5'- H_{b}), 3.93 (1 H, dd, $J = 2.7, 5.2$ Hz, 4'- H), 4.39 (1 H, ddd, $J = 2.3, 5.2, 6.0$ Hz, 3'- H), 6.32 (1 H, dd, $J = 5.7, 8.1$ Hz, 1'- H), 7.43 (1 H, s, 6- H), 7.43–7.46 (2 H, m, ArH), 7.53–7.58 (1 H, m, ArH), 7.94–7.97 (2 H, m, ArH), 8.35 (1 H, br s, NH). $^{13}\text{C NMR}$ (90 MHz, CDCl_3) δ -5.4, -5.4, -4.8, -4.7 ((CH_3)₂Si), 18.0, 18.4 ((CH_3)₃CSi), 25.7, 25.9 ((CH_3)₃CSi), 27.1 (7), 28.3 (8), 28.6 (9), 29.3 (10), 41.2 (2'), 63.1 (5'), 72.3 (3'), 84.9 (1'), 87.8 (4'), 114.7 (5), 127.2, 128.5 (Ar), 133.2 (6), 135.7, 137.1 (Ar), 150.0 (2), 163.0 (4), 191.8 (Ar). IR (film; NaCl) ν 2954, 2930, 1695, 1668, 1471, 1207, 1095, 886 cm^{-1} . FAB MS (3-NBA) m/z 649 ($\text{M}^+ + 1$).

C^5 -(Thiobenzoyl)-2'-deoxyuridine (10a). Compound **9a** (1.17 g, 1.90 mmol) was dissolved in THF (40 mL), and *n*-tetrabutylammonium fluoride monohydrate (1.80 g, 6.9 mmol, 3.5 equiv) was added. The reaction mixture was stirred under N_2 for 3 h after which the solvent was removed under reduced pressure to give a pink solid. The residue was chromatographed on silica gel (eluting with 65:5:30 $\text{CH}_2\text{Cl}_2/\text{MeOH}/$

petroleum ether) to afford **10a** (0.65 g, 90% yield) as a white foam. TLC (7:1:2 $\text{CH}_2\text{Cl}_2/\text{MeOH}/\text{petroleum ether}$) $R_f = 0.44$. $^1\text{H NMR}$ (360 MHz, $\text{CD}_3\text{CN}/\text{CDCl}_3$) δ 2.06–2.21 (2 H, m, 2'- $H_{\text{a,b}}$), 2.55–2.66 (2 H, m, 7- $H_{\text{a,b}}$), 3.18–3.24 (2 H, m, 8- $H_{\text{a,b}}$), 3.69 (2 H, d, $J = 3.1$ Hz, 5'- $H_{\text{a,b}}$), 3.84 (1 H, dd, $J = 3.2, 6.7$ Hz, 4'- H), 4.36–4.40 (1 H, m, 3'- H), 6.16 (1 H, t, $J = 6.6$ Hz, 1'- H), 7.41–7.46 (2 H, m, ArH), 7.54–7.58 (1 H, m, ArH), 7.75 (1 H, s, 6- H), 7.87–7.90 (2 H, m, ArH), 9.23 (1 H, s, NH). $^{13}\text{C NMR}$ (90 MHz, $\text{CD}_3\text{CN}/\text{CDCl}_3$) δ 26.4 (7), 26.9 (8), 39.4 (2'), 60.9 (5'), 69.8 (3'), 84.4 (1'), 86.6 (4'), 111.2 (5), 126.3, 128.0, 132.8, 136.2 (Ar), 137.2 (6), 149.6 (2), 162.6 (4), 190.8 (SCOPh). IR (film; NaCl) ν 3407, 2935, 1667, 1469, 1275, 1207, 1094, 916, 690 cm^{-1} . FAB MS (3-NBA) m/z 393 ($\text{M}^+ + 1$).

C^5 -(Thiobenzoyl)-2'-deoxyuridine (10b). Compound **9b** (0.90 g, 1.39 mmol) and *n*-tetrabutylammonium fluoride monohydrate (1.27 g, 4.84 mmol, 3.5 equiv) were dissolved in THF (28 mL). The reaction mixture was stirred under N_2 for 3 h after which the solvent was removed under reduced pressure. The residue was chromatographed on silica gel (eluting with 5% MeOH in CH_2Cl_2) to afford **10b** (0.60 g, 100% yield) as a white foam. TLC (10% MeOH in CH_2Cl_2) $R_f = 0.35$. $^1\text{H NMR}$ (360 MHz, CD_3OD) δ 1.71–1.75 (4 H, m, 8- $H_{\text{a,b}}$, 9- $H_{\text{a,b}}$), 2.31–2.35 (2 H, m, 2'- $H_{\text{a,b}}$), 2.43 (2 H, t, $J = 6.2$ Hz, 7- $H_{\text{a,b}}$), 3.14–3.18 (2 H, m, 10- $H_{\text{a,b}}$), 3.82 (1 H, dd, $J = 3.6, 12.0$ Hz, 5'- H_{a}), 3.89 (1 H, dd, $J = 3.1, 12.0$ Hz, 5'- H_{b}), 4.01 (1 H, dd, $J = 3.3, 6.5$ Hz, 4'- H), 4.50 (1 H, ddd, $J = 3.8, 6.5, 8.9$ Hz, 3'- H), 6.38 (1 H, t, $J = 6.7$ Hz, 1'- H), 7.53–7.58 (2 H, m, ArH), 7.66–7.68 (1 H, m, ArH), 7.94 (1 H, s, 6- H), 8.00–8.03 (2 H, m, ArH). $^{13}\text{C NMR}$ (90 MHz, CD_3OD) δ 27.2 (7), 28.6 (8), 29.4 (9), 30.2 (10), 41.2 (2'), 62.8 (5'), 72.2 (3'), 86.4 (1'), 88.8 (4'), 115.3 (5), 128.0, 129.8 (Ar), 134.5 (6), 138.4 (Ar), 152.2 (2), 165.9 (4), 193.4 (SCOPh). IR (KBr) ν 2949, 2869, 1724, 1656, 1272, 1096, 916, 689 cm^{-1} . FAB MS (3-NBA) m/z 421 ($\text{M}^+ + 1$).

5'-*O*-(4,4'-Dimethoxytrityl)- C^5 -(thiobenzoyl)-2'-deoxyuridine (11a). Compound **10a** (0.27 g, 0.71 mmol) was dissolved in pyridine (5 mL), the mixture was cooled to 0 °C, and 4,4'-dimethoxytrityl chloride (0.29 g, 0.85 mmol, 1.2 equiv) was added. The reaction mixture was stirred under N_2 for 6 h and the excess 4,4'-dimethoxytrityl chloride was then quenched with MeOH (1 mL). The solvent was removed under reduced pressure; the residue was coevaporated once with CH_3CN and chromatographed on silica gel (eluting with a step gradient of 33–100% Et_2O in petroleum ether) to afford **11a** (0.36 g, 75% yield) as a white foam. TLC (65:5:30 $\text{CH}_2\text{Cl}_2/\text{MeOH}/\text{petroleum ether}$) $R_f = 0.42$. $^1\text{H NMR}$ (360 MHz, $\text{CD}_3\text{CN}/\text{CDCl}_3$) δ 2.37–2.55 (4 H, m, 2'- $H_{\text{a,b}}$, 7- $H_{\text{a,b}}$), 3.49–3.57 (2 H, m, 8- $H_{\text{a,b}}$), 3.99–4.02 (8 H, m, 5'- $H_{\text{a,b}}$, 2 OCH_3), 4.20 (1 H, dd, $J = 3.1, 6.6$ Hz, 4'- H), 4.63–4.67 (1 H, m, 3'- H), 6.46 (1 H, t, $J = 6.8$ Hz, 1'- H), 7.06–7.10 (4 H, m, ArH), 7.36–8.12 (14 H, m, 6- H , ArH), 9.27 (1 H, s, NH). $^{13}\text{C NMR}$ (90 MHz, $\text{CD}_3\text{CN}/\text{CDCl}_3$) δ 26.3 (7), 26.6 (8), 39.2 (2'), 54.2 (OCH_3), 62.7 (5'), 70.3 (3'), 84.3 (1'), 85.0 (4'), 86.5 ($\text{OC}(\text{Ph})_3$), 112.0 (Ar), 112.3 (5), 125.9, 126.1, 127.2, 127.9, 128.2, 129.2, 132.7, 135.9 (Ar), 136.9 (6), 149.2 (2), 157.8 (4), 189.8 (SCOPh). IR (film; NaCl) ν 3452, 1670, 1608, 1509, 1465, 1447, 1250, 1207, 1176, 1034 cm^{-1} .

5'-*O*-(4,4'-Dimethoxytrityl)- C^5 -(thiobenzoyl)-2'-deoxyuridine (11b). Compound **10b** (0.45 g, 1.00 mmol) was dissolved in pyridine (6 mL), the mixture was cooled to 0 °C, and 4,4'-dimethoxytrityl chloride (0.41 g, 1.20 mmol, 1.2 equiv) was added. The mixture was stirred under N_2 for 18 h after which the excess 4,4'-dimethoxytrityl chloride was quenched with MeOH (1 mL). The solvent was removed under reduced pressure and the residue then chromatographed on silica gel (eluting with a step gradient of 33–100% Et_2O in petroleum ether) to afford **11b** (0.43 g, 59% yield) as a tan foam. TLC (1:1 acetone/petroleum ether) $R_f = 0.42$. $^1\text{H NMR}$ (360 MHz, CD_3CN) δ 1.31–1.41 (4 H, m, 8- $H_{\text{a,b}}$, 9- $H_{\text{a,b}}$), 1.78–1.84 (1 H, m, 2'- H_{a}), 1.92–1.98 (1 H, m, 2'- H_{b}), 2.14–2.29 (2 H, m, 7- $H_{\text{a,b}}$), 2.84 (2 H, t, $J = 6.8$ Hz, 10- $H_{\text{a,b}}$), 3.26 (2 H, d, $J = 3.4$ Hz, 5'- $H_{\text{a,b}}$), 3.94 (1 H, br s, 3'- OH), 3.73 (6 H, s, 2 OCH_3), 3.91 (1 H, dd, $J = 3.5, 7.0$ Hz, 4'- H), 4.45–4.48 (1 H, m, 3'- H), 6.23 (1 H, t, $J = 6.8$ Hz, 1'- H), 6.84–6.86 (4 H, m, ArH), 7.19–7.92 (15 H, m, 6- H , ArH), 9.12 (1 H, br s, NH). $^{13}\text{C NMR}$ (90 MHz, CD_3CN) δ 27.3 (7), 28.7 (8), 29.2 (9), 29.9 (10), 40.8 (2'), 55.9 (OCH_3), 64.5 (5'), 72.1 (3'), 85.2 (1'), 86.8 (4'), 87.3 ($\text{OC}(\text{Ph})_3$), 114.1 (Ar), 115.2 (5), 127.9, 128.0, 128.9, 129.1, 129.8, 131.0 (Ar), 134.5 (6), 136.7, 139.9, 138.0, 145

(Ar), 151.3 (2), 159.7 (Ar), 164.3 (4), 192.5 (SCOPH). IR (film; NaCl) ν 3427, 3060, 2935, 1665, 1509, 1257, 1032, 691 cm^{-1} . FAB MS (3-NBA) m/z 722 ($M^+ + 1$).

5'-O-(4,4'-Dimethoxytrityl)-C⁵-(ethyl)-2'-deoxyuridine tert-Butyl Disulfide (12a). Compound **11a** (0.77 g, 1.23 mmol) was dissolved in a MeOH/THF solution (3:1, 12 mL), and 1-(tert-butylthio)-1,2-hydrazinedicarboxymorpholide²⁷ (0.56 g, 1.61 mmol, 1.3 equiv) and LiOH·H₂O (0.16 g, 3.69 mmol, 3.0 equiv) were added. The reaction mixture was stirred under N₂ for 30 min, then diluted in Et₂O and washed with brine. The organic layer was dried over Na₂SO₄, concentrated under reduced pressure, and chromatographed on silica gel (eluting with 1:2 EtOAc/petroleum ether) to afford **12a** (0.67 g, 90% yield) as a colorless glass. TLC (65:5:30 CH₂Cl₂/MeOH/petroleum ether) R_f = 0.42. ¹H NMR (300 MHz, CD₃CN) δ 1.24 (9 H, s, C(CH₃)₃), 2.22–2.31 (4 H, m, 2'-H_{a,b}, 7-H_{a,b}), 2.63–2.69 (2 H, m, 8-H_{a,b}), 3.27 (2 H, d, J = 3.8 Hz, 5'-H_{a,b}), 3.76 (6 H, s, 2 OCH₃), 3.92 (1 H, dd, J = 3.7, 7.5 Hz, 4'-H), 4.42 (1 H, dd, J = 5.0, 8.9 Hz, 3'-H), 6.22 (1 H, t, J = 6.7 Hz, 1'-H), 6.84–6.89 (4 H, m, ArH), 7.22–7.45 (14 H, m, 6-H, ArH). ¹³C NMR (75 MHz, CD₃CN) δ 28.3 (7), 30.4 (C(CH₃)₃), 39.9 (8), 41.0 (2'), 48.5 (C(CH₃)₃), 56.1 (OCH₃), 64.9 (5'), 72.3 (3'), 85.7 (1'), 87.0 (4'), 87.5 (OC(Ph)₃), 113.2 (5), 114.3, 128.0, 128.9, 129.2, 131.1, 137.0 (Ar), 137.9 (6), 145.9 (Ar), 151.3 (2), 159.9 (Ar), 164.1 (4). IR (film; NaCl) ν 2960, 2931, 1696, 1684, 1674, 1654, 1508, 1250, 1199, 1177 cm^{-1} . FAB MS (3-NBA) m/z 681 ($M^+ + 1$).

5'-O-(4,4'-Dimethoxytrityl)-C⁵-(butyl)-2'-deoxyuridine tert-Butyl Disulfide (12b). Compound **11b** (0.40 g, 0.56 mmol) was dissolved in a MeOH/THF solution (3:1, 5.6 mL), and 1-(tert-butylthio)-1,2-hydrazinedicarboxymorpholide²⁷ (0.25 g, 0.72 mmol, 1.3 equiv) and LiOH·H₂O (0.07 g, 1.67 mmol, 3.0 equiv) were added. The reaction mixture was stirred under N₂ for 90 min, then diluted in Et₂O and washed with brine. The organic layer was dried over Na₂SO₄, the solvent removed under reduced pressure, and the residue chromatographed on silica gel (eluting with 3:2 petroleum ether:acetone) to afford **12b** (0.27 g, 69% yield) as a colorless glass. TLC (1:1 petroleum ether/acetone) R_f = 0.50. ¹H NMR (360 MHz, CD₃CN) δ 1.26 (9 H, s, C(CH₃)₃), 1.29–1.38 (4 H, m, 8-H_{a,b}, 9-H_{a,b}), 1.73–1.80 (1 H, m, 2'-H_b), 1.90–1.96 (1 H, m, 2'-H_b), 2.22–2.28 (2 H, m, 7-H_{a,b}), 2.46–2.50 (2 H, m, 10-H_{a,b}), 3.26–3.27 (2 H, m, 5'-H_{a,b}), 3.75 (6 H, s, 2 OCH₃), 3.91 (1 H, dd, J = 3.4, 6.7 Hz, 4'-H), 4.47 (1 H, br s, 3'-H), 6.23 (1 H, t, J = 6.8 Hz, 1'-H), 6.85–6.87 (4 H, m, ArH), 7.23–7.44 (14 H, m, 6-H, ArH), 9.17 (1 H, br s, NH). ¹³C NMR (90 MHz, CD₃CN) δ 27.3 (7), 28.5 (8), 29.7 (9), 30.2 (10, C(CH₃)₃), 40.9 (2'), 48.2 (C(CH₃)₃), 55.9 (OCH₃), 64.5 (5'), 72.1 (3'), 85.2 (1'), 86.8 (4'), 87.3 (OC(Ph)₃), 114.1 (Ar), 115.3 (5), 128.0, 128.9, 129.1, 131.0, 131.0, 136.6 (Ar), 136.8 (6), 145.8 (Ar), 151.3 (2), 159.7 (Ar), 164.3 (4). IR (film; NaCl) ν 2986, 2262, 1709, 1685, 1510, 1251, 1034, 832 cm^{-1} . FAB MS (3-NBA) m/z 707 ($M^+ + 1$).

3'-O-(N,N-Diisopropyl- β -cyanoethylphosphoramidite)-5'-O-(4,4'-dimethoxytrityl)-C⁵-(ethyl)-2'-deoxyuridine tert-Butyl Disulfide (13a). Compound **12a** (0.36 g, 0.52 mmol) was dissolved in CH₂Cl₂ (3 mL) containing *N,N*-diisopropylethylamine (0.46 mL, 2.62 mmol, 5.0 equiv) and cooled to 0 °C under a N₂ atmosphere. Chloro-*N,N*-diisopropylamino- β -cyanoethylphosphine (0.17 mL, 0.78 mmol, 1.5 equiv) was added dropwise and the reaction mixture was stirred warming to room temperature for 1 h. The excess chloridate was quenched with MeOH (1 mL) and the mixture was diluted with EtOAc and washed with saturated NaHCO₃ and brine. The organic layer was dried over Na₂SO₄, concentrated under reduced pressure, and chromatographed on silica gel (eluting with 60:35:5 EtOAc/petroleum ether/Et₃N) to afford **13a** (0.34 g, 74% yield) as a white foam. TLC (70:25:5 EtOAc/petroleum ether/Et₃N) R_f = 0.50, 0.58; two diastereomers. ¹H NMR (300 MHz, CD₃CN) δ (two diastereomers) 0.99–1.16 (12 H, m, 2 NCH(CH₃)₂), 1.22 (9 H, s, C(CH₃)₃), 2.22–2.38 (2 H, m, 2'-H_{a,b}), 2.40–2.52 (2 H, m, 7-H_{a,b}), 2.58–2.74 (4 H, m, OCH₂CH₂CN, 8-H_{a,b}), 3.25–3.35 (2 H, m, 5'-H_{a,b}), 3.50–3.70 (4 H, m, OCH₂CH₂CN, 2 NCH(CH₃)₂), 3.75 (6 H, s, 2 OCH₃), 4.02–4.10 (1 H, m, 4'-H), 4.50–4.62 (1 H, m, 3'-H), 6.23 (1 H, dd, J = 3.2, 6.7 Hz, 1'-H), 6.81–6.88 (4 H, m, ArH), 7.19–7.44 (10 H, m, 6-H, ArH). ¹³C NMR (75 MHz, CD₃CN) δ (two diastereomers) 20.9, 21.1 (OCH₂CH₂CN), 24.9, 25.0 (NCH(CH₃)₂), 27.9, 28.1 (7), 30.3 (C(CH₃)₃), 39.7 (8), 44.2 (2'), 44.3, 48.4 (C(CH₃)₃), 56.0 (OCH₃), 59.4 (OCH₂CH₂CN), 59.7, 64.3, 64.4 (5'), 74.5, 73.8 (3'),

85.6 (1'), 86.0 (4'), 87.5 (OC(Ph)₃), 113.2 (5), 114.2, 127.9, 131.0, 136.8 (Ar), 137.7 (6), 145.7 (Ar), 151.1 (2), 159.8 (Ar), 163.8 (4). ³¹P NMR (202 MHz; CD₃CN) δ 145.88, 145.91. IR (film; NaCl) ν 2964, 1690, 1609, 1510, 1463, 1364, 1251, 1178, 1085, 1038, 978, 832, 793, 726 cm^{-1} . FAB MS (3-NBA) m/z 881 ($M^+ + 1$). Anal. Calcd for C₄₅H₅₉N₄O₁₀PS₂: C, 61.47; H, 6.78; N, 6.37. Found: C, 61.50; H, 6.73; N, 6.41.

3'-O-(N,N-Diisopropyl- β -cyanoethylphosphoramidite)-5'-O-(4,4'-dimethoxytrityl)-C⁵-(butyl)-2'-deoxyuridine tert-Butyl Disulfide (13b). Compound **12b** (0.24 g, 0.34 mmol) was dissolved in CH₂Cl₂ (1.4 mL) containing *N,N*-diisopropylethylamine (0.30 mL, 1.70 mmol, 5.0 equiv) and cooled to 0 °C under a N₂ atmosphere. Chloro-*N,N*-diisopropylamino- β -cyanoethylphosphine (0.13 mL, 0.51 mmol, 1.5 equiv) was added dropwise and the mixture was stirred while warming to room temperature for 20 min. The excess chloridate was quenched with MeOH (1 mL) and the reaction mixture was diluted with EtOAc and washed with saturated NaHCO₃ and brine. The organic layer was dried over Na₂SO₄, the solvents were removed under reduced pressure, and the residue was chromatographed on silica gel (eluting with a step gradient of 20–40% acetone in petroleum ether) to afford **13b** (0.29 g, 94% yield) as a white foam. TLC (1:1 acetone/petroleum ether) R_f = 0.71. ¹H NMR (360 MHz, CD₃CN) δ (two diastereomers) 1.02–1.19 (12 H, m, NCH(CH₃)₂), 1.26 (9 H, s, C(CH₃)₃), 1.20–1.36 (4 H, m, 8-H_{a,b}, 9-H_{a,b}), 1.76–1.84 (1 H, m, 2'-H_a), 1.90–2.00 (1 H, m, 2'-H_b), 2.32–2.47 (2 H, m, OCH₂CH₂CN), 2.46 (2 H, t, J = 6.8 Hz, 7-H_{a,b}), 2.62 (2 H, t, J = 7.0 Hz, 10-H_{a,b}), 3.25–3.40 (2 H, m, 5'-H_{a,b}), 3.40–3.65 (4 H, m, OCH₂CH₂CN, 2 NCH(CH₃)₂), 3.87 (6 H, s, 2 OCH₃), 3.98–4.11 (1 H, m, 4'-H), 4.59–4.70 (1 H, m, 3'-H), 6.27 (1 H, dd, J = 3.3, 6.7 Hz, 1'-H), 6.81–6.88 (4 H, m, ArH), 7.22–7.44 (10 H, m, 6-H, ArH), 9.47 (1 H, br s, NH). ¹³C NMR (75 MHz, CD₃CN) δ (two diastereomers) 20.6, 21.0 (OCH₂CH₂CN), 24.9, 25.0 (NCH(CH₃)₂), 27.3 (7), 28.6 (8), 30.0 (9), 30.3 (10, C(CH₃)₃), 41.0 (2'), 48.3 (C(CH₃)₃), 56.0 (OCH₃), 59.3, 59.4 (OCH₂CH₂CN), 64.0, 64.2 (5'), 74.5, 73.8 (3'), 85.3 (1'), 86.1 (4'), 87.4 (OC(Ph)₃), 114.2 (Ar), 115.6 (5), 118.4, 128.1, 129.0, 129.1, 129.2, 131.1, 136.6 (Ar), 136.9 (6), 145.8 (Ar), 151.5 (2), 159.8 (Ar), 164.5 (4). ³¹P NMR (202 MHz; CD₃CN) δ 145.77. IR (film; NaCl) ν 2967, 1707, 1685, 1509, 1250, 1179, 1034, 978, 829 cm^{-1} . FAB MS (3-NBA) m/z 906 ($M^+ + 1$). Anal. Calcd for C₄₇H₆₃N₄O₁₀PS₂: C, 62.22; H, 7.01; N, 6.18. Found: C, 61.82; H, 6.91; N, 6.11.

Nucleic Acid Synthesis. Solid-phase DNA synthesis was conducted on a Millipore Expedite 8909 DNA/RNA synthesizer using dA^N-Bz, dC^N-Bz, dG^N-ibu, and dT *N,N*-diisopropylamino- β -cyanoethyl phosphoramidites following the manufacturer's protocols. Average coupling efficiencies were >98.5%. High performance liquid chromatography (HPLC) was performed using either a Waters Associates Model 600 chromatograph coupled to a Waters Model 484 absorbance detector (260 nm) for peak detection or a Waters Model 510 chromatograph coupled to a Waters Model 441 absorbance detector (254 nm) for peak detection. Unless otherwise noted, purification of oligodeoxynucleotides was conducted using Vydac C₄ columns (4.6 × 250 mm for analysis, 1 mL/min, and 7.9 × 250 mm for preparative runs, 4 mL/min) and triethylammonium acetate (TEAA, 0.1 M, pH 6.6) and CH₃CN as the mobile phases. All sequences were ion-exchanged into the sodium form prior to analysis by incubation in NaCl (4 M) overnight at 4 °C. The excess salt was removed by reversed-phase HPLC (step gradient of 100% H₂O–0% CH₃CN in 7 min to 80% H₂O–20% CH₃CN in 15 min). After purification all sequences were >99% pure as judged by HPLC and denaturing PAGE (20% polyacrylamide gels (19:1) containing 8 M urea). Molar extinction coefficients (ϵ_{260} , M⁻¹ cm⁻¹) were determined by phosphate analysis as described by Snell and Snell⁵⁶ and are 287 000 for I, 286 000 for II, 285 000 for III, 274 000 for IV, and 274 000 for V.

tert-Butyl Protected Triplexes II and III. Derivatized supports containing the N³-(thioethyl)thymidine (N³S)^{12,13} (29 mg, 1 μ mol) were loaded into empty reaction cartridges and elongated to give the sequences shown in Figure 3 (the terminal trityl group was not removed). Amidite **13a** or **13b** was added through the 5-nucleotide port on the synthesizer during the requisite coupling step. After the

(56) Snell, F. D.; Snell, C. T. *Colorimetric Methods of Analysis*, 3rd ed.; Van Nostrand: New York, 1949; Vol. 2, p 671.

syntheses were complete, the resins were removed from the reaction columns and suspended in concentrated NH_4OH (0.5 mL). After 1 h the supports were pelleted by centrifugation, and the supernatants were removed and washed with fresh NH_4OH (0.5 mL). After an additional 7 h at 55 °C the NH_4OH was removed *in vacuo*. The residues were dissolved in water (2 mL) and purified by reversed-phase HPLC (linear gradient of 85% TEAA–15% CH_3CN to 25% CH_3CN in 60 min). Retention times are 25.0 min for II and 24.8 min for III. The fractions that contained the products were pooled and concentrated *in vacuo*. The 5'-trityl group on each sequence was removed by incubating with 80% AcOH (1 mL) at room temperature. After 20 min the reactions were quenched with EtOH (0.2 mL) and the solvents were removed *in vacuo*. The *tert*-butyl thiol protected modified sequences were purified by reversed-phase HPLC (linear gradient of 95% TEAA–5% CH_3CN to 20% CH_3CN in 60 min) to give 3.63 mg (0.34 μmol , 34% yield) of II or 4.37 mg (0.42 μmol , 42% yield) of III. Retention times are 33.0 min for II and 36.6 min for III.

Cross-Linked Triplexes IV and V. Reduction of the *tert*-butyl protected triplexes was performed by dissolving the DNAs in buffer (0.1 M NaH_2PO_4 , [DNA] = 1 mM, pH 8.3) containing DTT (250 equiv) followed by incubation at 37 °C. After 4 h, the reductions were complete as judged by reversed-phase HPLC and the reduced sequences were separated from excess DTT by reversed-phase HPLC (linear gradient of 93% TEAA–7% CH_3CN to 22% CH_3CN in 60 min). Retention times are 18.0 min for IV and 20.2 min for V. The solvent was removed *in vacuo* and the DNAs were each dissolved in PBS³¹ containing MgCl_2 (5 mM) ([DNA] = 0.5 mM, pH 7.25) and vigorously stirred for 24 h at 25 °C exposed to the atmosphere. Every 4 h an aliquot (3 μL) was removed from the reaction mixtures, examined by HPLC, and tested for the presence of free thiol groups by Ellman's reagent. After 24 h, the reactions were judged complete. The mixtures were then acidified to pH 3 with AcOH and the cross-linked triplexes were purified by reversed-phase HPLC (linear gradient of 93% TEAA–7% CH_3CN to 22% CH_3CN in 60 min) to give 2.84 mg (0.27 μmol , 27% yield) of IV or 3.02 mg (0.29 μmol , 29% yield) of V. Retention times are 14.2 min for IV and 16.0 min for V.

Nucleoside Composition Analysis. DNA samples (0.4 OD_{260} U) were dissolved in water (to 370 μL). Dephosphorylation buffer (50 μL , 500 mM TRIS-HCl, 1 mM EDTA, pH 8.5), calf intestine alkaline phosphatase (50 μL , 50 U), and phosphodiesterase from *Crotalus durissus* (30 μg) were added and the mixtures were incubated at 37 °C for 12 h. Aliquots of the reaction mixtures (50 μL) were filtered through an Amicon Microcon-3 filter (Beverly, MA) to remove the protein and were analyzed by HPLC (convex gradient of 100% TEAA–0% CH_3CN to 15% CH_3CN in 60 min, then linear gradient to 90% CH_3CN in 30 min) using a Waters $\mu\text{Bondapak C}_{18}$ column (3.8 \times 300 mm, 1 mL/min) and peaks quantitated via a Shimadzu Model C-R6A

integrator assuming nucleoside extinction coefficients^{10d,13} (ϵ_{254} , $\text{M}^{-1}\text{cm}^{-1}$) of 13 300, for dA; 6300 for dC; 13 000 for dG; 6600 for T; 6200 for $\text{N}^3\text{S}_{\text{tBu}}$; 7100 for $\text{C}^5\text{S}_{\text{tBu}}$; and $\text{C}^5\text{S}_{\text{tBu}}$; and 10 500 for $\text{N}^3\text{S}-\text{C}^5\text{S}$ and $\text{N}^3\text{S}-\text{C}^5\text{S}$. Retention times (min) are 10.0 for dC; 28.4 for T; 33.6 for dG; 47.2 for dA; 66.0 for $\text{N}^3\text{S}-\text{C}^5\text{S}$; 67.1 for $\text{N}^3\text{S}-\text{C}^5\text{S}$; 76.9 for $\text{C}^5\text{S}_{\text{tBu}}$; 77.6 for $\text{C}^5\text{S}_{\text{tBu}}$; 79.5 for $\text{N}^3\text{S}_{\text{tBu}}$.

Circular Dichroism. CD spectra were measured at 20 °C on an AVIV 62DS spectrometer equipped with a thermoprogrammable peltier. The DNA samples were dissolved in 0.1-cm long self-masking cuvettes with PBS (0.1 mL) containing MgCl_2 (0.5 mM) to a strand concentration of ~ 10 μM and pH adjusted with either HCl (1 N) or NaOH (1 N). The wavelength was scanned from 350 to 205 nm with a step size of 0.5 nm, bandwidth of 1.5 nm, and signal averaging time of 1.0 s. Each scan was repeated five times with the resultant average plot smoothed using manufacturers' protocols ($\delta/\delta^2 \leq 2.25$). To facilitate comparisons, the spectra were normalized to θ (molar ellipticity) based on dynode voltage at 260 nm using the ϵ_{260} values for each sequence.

Nuclear Magnetic Resonance Spectroscopy. Spectra were measured on a Bruker AMX 500 MHz NMR. DNA samples were dissolved in PBS buffer containing MgCl_2 (0.5 mM) (500 μL , 90% $\text{H}_2\text{O}/10\%$ D_2O) and pH adjusted with either HCl (1 N) or NaOH (1 N) to final concentrations of 1.0 mM. The samples were heat-denatured and slowly renatured prior to analysis. One dimensional spectra were recorded using a 1₁ solvent suppression scheme⁵⁷ with a 71.4 μs delay between pulses and were processed with a line broadening of 4.2 Hz. The imino protons were assigned from NOESY spectra ($\tau_m = 100$ ms) measured at 1 °C and 37 °C and pH 6.0 with a 1₁ solvent suppression scheme.⁵⁷ The data were transferred to a Silicon Graphics work station and processed using the FELIX software (Biosym Technologies). All spectra were convoluted in the time dimension in order to reduce the intensities of the water resonance.

Acknowledgment. This work was supported by NIH Grant GM 53861. G.D.G. is the recipient of a National Arthritis Foundation Arthritis Investigator Award, an American Cancer Society Junior Faculty Research Award, a National Science Foundation Young Investigator Award, a Camille Dreyfus Teacher-Scholar Award, and a research fellowship from the Alfred P. Sloan Foundation.

Supporting Information Available: CD spectra as a function of pH and spectra from the NMR melting experiments as a function of pH (6 pages). See any current masthead page for ordering and Internet access instructions.

JA963285H

(57) Plateau, P.; Guéron, M. *J. Am. Chem. Soc.* **1982**, *104*, 7310–7311.